Organelle biogenesis on a synthetic bead

Chia-Chun Chang*[1,2], Min Peng*[1], Lorena Blaya-Martinez[1,3], Siu-Shing Wong[1], Nada Mohamad[1], Bocheng Xiao[1], Joao M. Monteiro[1,4], Tess Harrison[1,5], Jordan W. Raff[1§]

[1]The Sir William Dunn School of Pathology, University of Oxford; Oxford, OX1 3RE, UK.

[2]Department of Animal Science and Technology, National Taiwan University; Taipei City, 106 Taiwan.

Present address:

[3]The Gurdon Institute, University of Cambridge; Cambridge CB2 1QN, UK.

[4]Department of Biochemistry, University of Oxford; Oxford, OX1 3QU, UK.

[5] ICFO, Avinguda Carl Friedrich Guass, Barcelona, Spain

*These authors contributed equally to this work

[§]Correspondence: jordan.raff@path.ox.ac.uk

Keywords: Centriole, Centrosome, Organelle, Biogenesis, Drosophila, Cell Cycle

Abstract

Centrosomes are complex organelles that comprise multiple copies of hundreds of different proteins, yet they can precisely duplicate every cell cycle. Here we reconstitute centrosome duplication on synthetic beads programmed to recruit core centrosome assembly proteins when injected into *Drosophila* embryos. These beads generate structures that are functionally indistinguishable from centrosomes: they recruit centriole/centrosome proteins, organise microtubules (MTs) and proceed through multiple rounds of high-fidelity duplication, all in synchrony with the endogenous centrosomes. The beads function as seeds that recruit biogenesis-promoting proteins to stimulate the assembly of relatively simple scaffolds that direct centrosome self-assembly. This “Seed—Scaffold—Self-Assemble” mechanism may represent a general principle of organelle biogenesis, explaining how simple molecular inputs can generate complex structures without the need to copy a pre-existing template.

Main Text

Cells contain many organelles that perform a myriad of functions. How cells build such complicated structures and regulate their biogenesis to maintain homeostasis is poorly understood (*1–3*). Centrosomes are an attractive model for studying organelle biogenesis as their number, shape and size are tightly controlled (*4–6*). Most cells inherit a single centrosome, comprising a mother-daughter centriole pair surrounded by Pericentriolar Material (PCM), which duplicates once per cell cycle (Fig.1A). To understand how these structures assemble we analysed early *Drosophila* embryos, where centrosomes undergo 13 rounds of rapid and near-synchronous duplication in a common cytoplasm (*7*). Here, putative molecular pathways of daughter centriole and PCM assembly have been defined (Fig.1B) (*8*, *9*). To initiate centriole or PCM assembly, a protein that forms a torus around the mother centriole (Asl or Ana1, respectively, *yellow*, Fig.1B) recruits a protein kinase (Plk4 or Polo/PLK1, respectively, *light/dark blue*, Fig.1B). Plk4 breaks symmetry and phosphorylates Ana2 to initiate the assembly of an Ana2/Sas-6/Sas-4 scaffold that supports daughter centriole assembly at a single site on the side of the mother (*10–15*) (*orange*, Fig.1B); Polo/PLK1 phosphorylates Spd-2 to initiate the assembly of a Spd-2/Cnn/TACC scaffold that supports PCM assembly around the mother (*16*, *17*) (*brown*, Fig.1B).

Synthetic beads bound to Sas-6 and Ana2 can recruit PCM and organise MTs

We wondered whether a synthetic bead, programmed to recruit one or more of these core assembly proteins, could replace the mother centriole as a platform to support daughter centriole and/or PCM biogenesis. To test this, we coupled biotinylated anti-GFP Nanobodies to 1µm streptavidin magnetic beads (Fig.1C). We injected these beads into early embryos expressing Jupiter-mCherry (Jup-mCh) as a MT marker and

various GFP-fusions that would bind to the beads—using a magnet to position the beads at the embryo cortex so we could compare their behaviour to the endogenous centrosomes that arrive at the embryo cortex during nuclear cycle 10 (Fig.1C).

We first injected these beads into embryos expressing Sas-6-GFP and Ana2-GFP as, when co-overexpressed in embryos, these proteins can assemble into **S**as-6/**A**na2 **p**articles (**SAPs**) that recruit centrosome proteins and organise MTs (*18*). The beads bound the GFP-fusions and, in contrast to controls, they often organised MTs (Fig.1D,E; Fig.S1). We then generated Sas-6/Ana2-beads in embryos co-expressing red-fluorescent-fusions to other centrosome proteins. The beads recruited all these proteins in a manner that resembled their recruitment to centrosomes (*18*) (Fig.1F). Moreover, in *Drosophila* embryos, centrioles generate a pulse of Polo/PLK1 and Spd-2 recruitment during each nuclear cycle that drives a pulse of mitotic-PCM/MT recruitment (*19*); the Sas-6/Ana2-beads generated similar pulses, in phase with the endogenous centrosomes (Fig.1G). Thus, Sas-6/Ana2-beads organise MTs because they recruit PCM in an active manner that mimics the endogenous centrosomes.

Sas-6/Ana2-beads generate **C**entrosome-**Li**ke **P**article**s** (**CLiPs**)

We noticed that many Sas-6/Ana2-beads generated **C**entrosome-**Li**ke **P**article**s** (**CLiPs**) that separated from the bead surface as the endogenous centrosomes were separating at the end of mitosis (Fig.2A; Movie S1). Many of these CLiPs were functionally indistinguishable from centrosomes: they organised MTs, proceeded through multiple rounds of duplication (Fig.2A,B, Movie S1,S2), formed spindle poles (Fig.2C; Movie S3) and organised cortical actomyosin (Fig.S2; Movie S4)—all in synchrony with the endogenous centrosomes. Interestingly, the beads only generated

CLiPs once the endogenous centrosomes and nuclei arrived at the embryo cortex (Fig.S3; Movie S5), suggesting that the embryonic **C**ell **C**ycle **O**scillator (**CCO**)—which oscillates locally around the centrosomes and nuclei in these embryos (*20*, *21*)—is required to initiate CLiP assembly. In addition, some CLiPs contained low levels of Sas-6-GFP/Ana2-GFP and did not initially duplicate (e.g. *cyan arrow*, Fig.2A). These CLiPs often gradually increased in fluorescence intensity and duplicated in later cycles (Fig.S3; Movie S5). Thus, some CLiPs take time to "mature" to become duplication competent.

The ability of Sas-6/Ana2-beads to generate MTs and CLiPs was highly correlated: ~75-80% of the beads that organised MTs generated at least one, and usually multiple, CLiP(s) (N=9 embryos; 179 MT-generating beads analysed, 138 of which generated CLiPs), whereas we never observed a bead that did not organise MTs generate a CLiP. In the following experiments we quantified the ability of various fusion-protein-coupled beads to organise MTs; unless otherwise stated, most of the beads that organised MTs also generated CLiPs.

<u>Ana2-beads generate MTs and CLiPs by recruiting Sas-4</u>

To test whether any of the core centriole assembly proteins—Asl, Plk4, Sas-6, Ana2, Sas-4 or Ana1 (Fig.1B)—could individually generate MTs/CLiPs, we injected GFP-Nanobody beads into embryos expressing Jup-mCh and GFP-fusions of each individual protein expressed from their endogenous promoter. Ana2-GFP could be recruited to beads at much higher levels than the other proteins, and many of the beads that recruited higher-levels of Ana2 generated MTs/CLiPs (Fig.3A). Ana2 (STIL in humans) has a central role in centriole duplication (Fig.1B) as it is phosphorylated

by Plk4 to drive interactions with Sas-4/CPAP and Sas-6 that promote centriole scaffold assembly (*10–15*) (Fig.3B). To assess the importance of these interactions for MT/CLiP generation, we adapted our assay by coupling beads to an anti-ALFA-tag-Nanobody (*22*). We co-injected these beads with mRNA encoding ALFA-tagged fusions of WT or mutant versions of Ana2 that cannot self-interact (ΔCC) (*23*) or that cannot interact with Sas-4 (ΔCR2) (*24*, *25*) or Sas-6 (*10*, *11*) (ΔSTAN), into embryos expressing Jup-mCh and GFP/mNG-fusions to various centrosome proteins. We then assessed whether the beads recruited the GFP/mNG-fusion and/or generated MTs/CLiPs.

As a control, we confirmed that the non-fluorescent ALFA-tagged Ana2 bound to the beads by showing that Ana2-ALFA-beads could co-recruit Ana2-GFP (presumably by forming Ana2-ALFA::Ana2-GFP multimers), and this was abolished if Ana2-ALFA's homo-oligomerising domain was deleted (ΔCC, Fig.3C). C-terminally tagged Ana2 (WT-ALFA) beads also recruited Sas-4-NG and generated MTs/CLiPs but, surprisingly, N-terminally-tagged (ALFA-WT) Ana2 beads did not (Fig.3D)—even though both sets of beads could recruit Ana2-GFP (Fig.3C). Moreover, Ana2-ΔCC-ALFA-beads—that could not recruit Ana2-GFP (Fig.3C)—still recruited Sas-4 and generated MTs/CLiPs (Fig.3D). This suggests that Ana2-beads need to recruit Sas-4 to generate MTs/CLiPs. To test this, we coupled beads to different mutant forms of Ana2 that cannot interact with Sas-4—ΔCR2; P11A,R12A; S38A (*14*, *15*, *24*). These beads could all recruit Ana2-GFP (Fig.3E), but not Sas-4-NG, and they could not generate MTs/CLiPs (Fig.3F). In contrast, Ana2-beads that could not bind Sas-6 (Ana2-ΔSTAN) or could not bind Sas-6 or Ana2 (Ana2-ΔCC+ΔSTAN) still recruited

Sas-4 and generated MTs/CLiPs (Fig.3F). Thus, the ability of Ana2-beads to recruit Sas-4, but not Ana2 or Sas-6, seems to be crucial for MT/CLiP generation.

Beads coupled to one of several core centriole assembly proteins can generate CLiPs

This requirement for Sas-4 recruitment was perhaps surprising, as beads coupled directly to Sas-4-GFP expressed from its endogenous promoter did not generate MTs/CLiPs (Fig.3A). We wondered whether this was because the concentration of Sas-4 on the bead surface was too low. To test this, we injected GFP-Nanobody beads into embryos expressing Sas-4-GFP either from its endogenous promoter (eSas-4) or from the ubiquitin-promoter (uSas-4), which is expressed at ~2-5X higher levels (*26*). The uSas-4 beads recruited significantly more Sas-4 and now robustly generated MTs/CLiPs (Fig.4A; Movie S6). We therefore tested if the other core centriole assembly proteins could generate MTs/CLiPs if recruited to beads at higher concentrations—using either the ubiquitin-promoter or mRNA injection to drive higher levels of protein expression. We found that Asl, Ana1 and Sas-6 could all generate MTs/CLiPs if coupled to beads at a high enough concentration (Fig.4B-D; Movies S7-S9). In contrast, at the concentrations we were able to test, neither Plk4- nor Polo/PLK-1 beads generated MTs/CLiPs, although these beads recruited significant amounts of each protein compared to controls (Fig.4E,F; Movies S10, S11).

Beads engage the canonical centriole assembly pathway to generate CLiPs

To test whether beads generate CLiPs using the canonical centriole assembly pathway (illustrated in Fig.1B), we coupled beads to each individual CLiP-generating protein and monitored the recruitment of the other core pathway proteins. As an important control, we also tested Spd-2-coupled beads—as these beads recruit PCM

and MTs but do not generate CLiPs (*17*) (Fig.4G). All the CLiP-generating proteins recruited themselves and the other centriole pathway proteins to varying degrees compared to controls (*top panels*, Fig.4H; see Fig.S4 for full dataset), whereas Spd-2-beads did not (*bottom panels*, Fig.4H). Thus, the ability of beads to generate CLiPs, but not MTs, is correlated with their ability to recruit core centriole assembly proteins.

To further test whether the canonical centriole-assembly pathway was required for CLiP biogenesis, we took advantage of our previous observation that Sas-4 has an Ser_{199}-Thr_{200}-Pro_{201} motif that is phosphorylated on T_{200} by Cdk/Cyclins. This phosphorylation is required to recruit Polo to daughter centrioles, which allows daughters to mature into mothers that can recruit Asl, duplicate and recruit PCM (*26*). We coupled beads to mutant forms of Sas-4 that contained single amino-acid substitutions rendering Sas-4 either unable to be phosphorylated on T200 by Cdk/cyclins (T200A or P201G) or unable to recruit Polo when T200 is phosphorylated (S199G or S199T) (*26*). The mutant proteins were recruited to beads as efficiently as the WT protein (Fig.4I, left panel) but, strikingly, none of them could recruit Polo or Asl and none of them could generate MTs/CLiPs (Fig.4I, centre and right panels). Thus, the interactions that drive canonical centriole and PCM assembly at mother centrioles (Fig.1B) appear to drive CLiP and PCM assembly on the bead (Fig.5A).

<u>Plk4 is required to generate CLiPs, but not MTs</u>

A prediction of the pathway outlined in Fig.5A is that—uniquely amongst the core centriole assembly proteins—Plk4 is required for CLiP, but not PCM/MT, generation. Plk4 is initially recruited all around the mother centriole, but it breaks symmetry to form a single site for daughter centriole assembly (Fig.1B) (*27*). We recently modelled Plk4

symmetry-breaking as a Turing reaction-diffusion system in which Plk4 can potentially break-symmetry on any surface (*28*). In this model, the larger the surface, the more sites will be selected for daughter assembly, presumably explaining why these large 1µm beads often generate multiple CLiPs (Fig.5A). Plk4 is present at very low levels in *Drosophila* embryos (*29*) and, although we could visualise GFP-Plk4 being recruited to GFP-Plk4-Nanobody beads that did not generate MTs/CLiPs (Fig.4E; Movie S10), we were unable to visualise Plk4 on any beads that did generate MTs/CLiPs. Thus, if Plk4 is recruited to beads that generate MTs/CLiPs, it is recruited at low levels.

Kinase-dead Plk4 (Plk4-KD) cannot break symmetry, and it accumulates to high levels around the entire mother centriole (*30*–*32*). Plk4-KD-NG was detectable at Sas-6/Ana2-beads and, like WT Plk4 at centrosomes (*29*), it was recruited in a pulsatile manner (Fig.5B). In contrast, Spd-2-beads, which generate MTs but not CLiPs (Fig.4G), did not generate pulses of Plk4-KD-NG recruitment (Fig.5B). Thus, beads that generate CLiPs can recruit at least kinase-dead versions of Plk4 in a manner that mimics Plk4's normal recruitment to centrioles. To test whether Plk4 was required for CLiP generation, we generated CLiPs in embryos injected with Plk4 RNAi. In these embryos the endogenous centrioles quickly stopped duplicating, but the embryos continued to progress through additional nuclear cycles (Fig.5C; Movie S12). Strikingly, the beads in these embryos continued to generate MTs that cycled in synchrony with the MTs on the remaining endogenous centrioles, but the centrioles did not duplicate, and the beads did not generate CLiPs. Thus, as predicted (Fig.5A), Plk4 is required for beads to generate CLiPs, but not MTs.

CLiPs may be *bona fide* centrosomes

To assess whether CLiPs could be *bona fide* centrosomes, we generated CLiPs in embryos expressing red-fluorescent-fusions of various centriole- and centrosome-proteins and compared the fluorescence intensity at centrioles and CLiPs (Fig.5D,E). All the proteins we tested were recruited to CLiPs, but often at slightly lower levels than at endogenous centrosomes (Fig.5E). This may be because some CLiPs are initially not fully matured and are initially unable to duplicate (Fig.S3).

To assess whether CLiPs contain centrioles, we used super-resolution microscopy to examine CLiPs in living embryos expressing Jup-mCh and NG-Asl, as Asl normally forms a distinctive "torus" around the mother centriole (*33–35*). An Asl torus could be visualised at both the endogenous centrioles and at CLiPs as they moved around in the embryo, flipping between an end-on orientation (where the torus appears as a ring—*arrowheads*, magnified views, Fig.5F) and side-on orientation (where the torus appears as a thin bar—*arrows*, magnified views, Fig.5F) (Movie S13). The Asl torus had a slightly smaller average diameter at CLiPs than at centrioles (Fig.5G), which is consistent with our hypothesis that some CLiPs are not fully matured, as daughter centrioles increase in diameter as they mature (*36*). We conclude that CLiPs have a similar molecular composition to centrosomes and are centred around a barrel-shaped structure that has a similar shape to centrioles.

Discussion

Our findings indicate that, unlike DNA replication, canonical centrosome replication does not require a pre-existing structural template. Instead, the information to assemble a new centrosome appears to arise dynamically from self-organising molecular interactions. Remarkably, these interactions can be seeded by a synthetic bead programmed to recruit any one of several core centriole assembly proteins. These beads can generate centrosome-like-particles (CLiPs) that appear to be molecularly, structurally and functionally equivalent to centrosomes. We conclude that the local recruitment and activation of a small set of factors is sufficient to initiate a cascade of self-assembly that can build a highly complex organelle.

Our data suggests that to function as seeds, synthetic beads must recruit assembly factors in a manner that meets two criteria. First, they must recruit key biogenesis-initiating kinases in a way that activates them appropriately. Recruiting Polo/PLK1 and Plk4 directly to beads is not sufficient to stimulate organelle assembly, presumably because these kinases must be activated by their recruiting proteins to phosphorylate key scaffolding substrates and, in the case of Plk4, to break-symmetry. Second, the beads must recruit assembly factors at a high enough concentration to trigger scaffold, and ultimately organelle, self-assembly. This is presumably because a threshold local concentration of protein is required to initiate and maintain positive-feedback interactions that drive MT/CLiP generation. If these seeding conditions are met, then the information to guide subsequent organelle assembly appears to be largely encoded in the scaffold and organelle building blocks themselves.

Protein self-assembly is a fundamental organising principle in biology, underpinning structures from viral capsids to ribosomes (*37*, *38*), but our finding that these principles can guide the assembly of centrosomes is perhaps surprising, as centrosomes comprise 10s-100s of copies of probably several hundred different proteins (*39*). Importantly, the embryo appears to provide at least one additional source of information to guide assembly: the embryonic cell cycle oscillator (CCO). In fly embryos the CCO oscillates locally around the nuclei and centrosomes (*20*, *21*), and centrosomes can assemble in S-phase but not in mitosis. This presumably explains why beads cannot generate CLiPs until the endogenous centrosomes/nuclei are nearby, as the CCO generates alternating permissive (S-phase) and non-permissive (M-phase) environments that entrain centriole/CLiP and PCM assembly on the beads and at the endogenous centrosomes.

In addition to these global changes in kinase activity, we speculate that as centrioles/centrosomes assemble, the building blocks may further guide assembly by changing *local* kinase activity at centrioles/centrosomes. Many centriole/centrosome proteins recruit PLK1 in these embryos, including the key assembly proteins Sas-4, Ana1 and Spd-2 (*26*, *40*, *41*). So, as centrioles/centrosomes grow and incorporate more of these proteins, the local concentration of PLK1 should increase. Polo/PLK1 has a major role in regulating many aspects of centriole and centrosome biogenesis (*19*, *42–44*) so a gradual rise in local PLK1 activity could determine when various events occur during assembly. In this scenario, global cell cycle cues provide permissive "*when*" signals for assembly, while the building blocks themselves—and the local kinase fluctuations they potentially generate—provide instructive "*how*" signals.

Our findings define a simple design logic for centrosome assembly we term **Seed—Scaffold—Self-Assemble**: a specific **seed** appropriately concentrates enzymes and building blocks to generate a relatively simple **scaffold** upon which these organelles can **self-assemble**. Many cellular assemblies—from membraneless condensates to kinetochores to membrane-bound organelles that grow from specialised contact sites—seem to rely on local cellular cues to promote assembly (*45–48*) so this logic offers a parsimonious framework for organelle biogenesis more broadly. Importantly, the model explains how relatively simple molecular inputs can produce large, molecularly complex structures without the need to directly copy a pre-existing structural template. It will be important to understand how seeds, and the scaffolds they generate, shape the local reaction-diffusion landscapes to guide biogenesis. This may allow us to one day engineer complex self-assembling nanomachines comprising multiple copies of hundreds of different proteins.

Figure 1

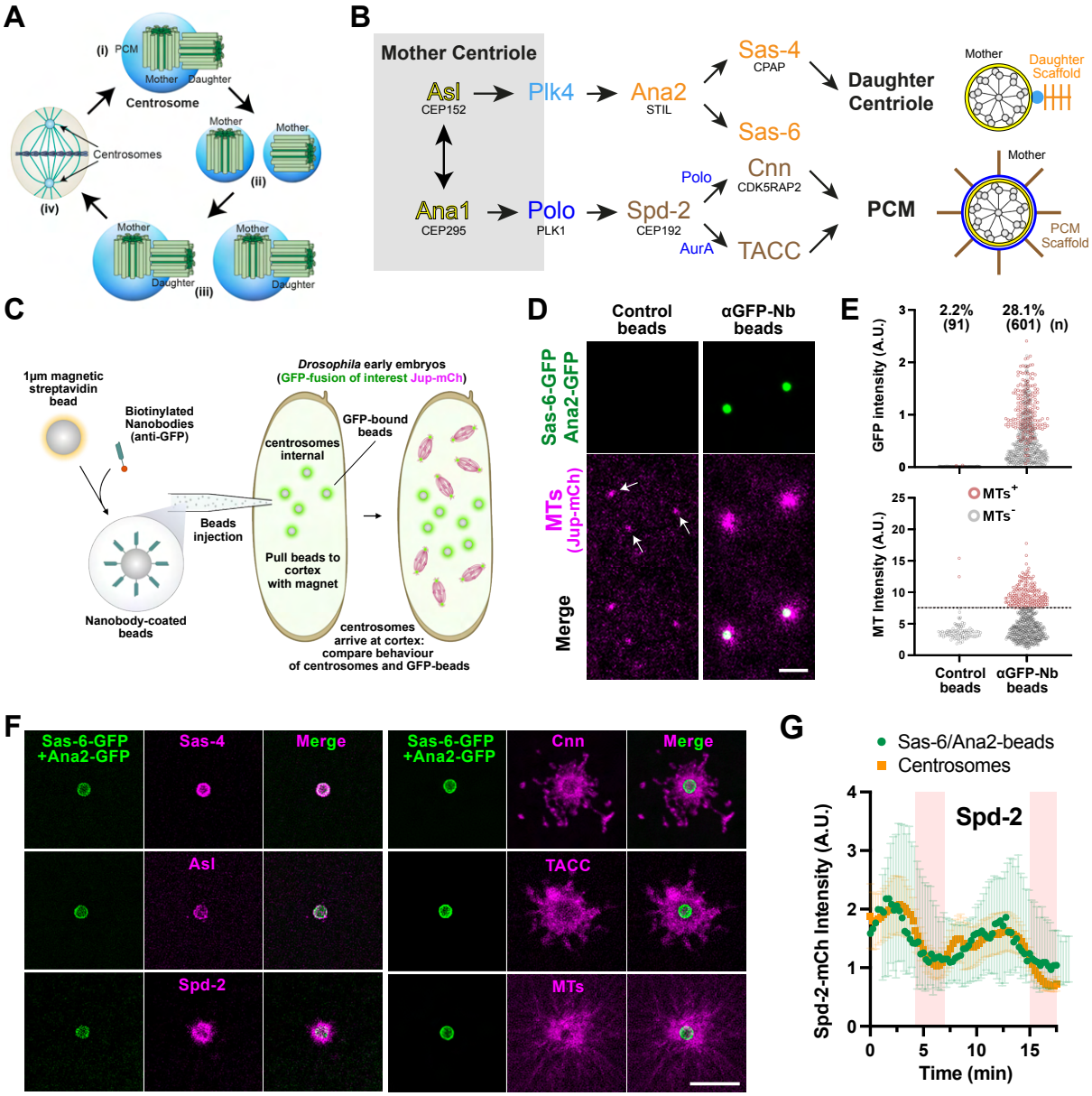
A
(i) PCM
Mother
Daughter
Centrosome
Centrosomes
(ii)
(iii)
(iv)
B
Mother Centriole
Asl
CEP152
Plk4
Ana2
STIL
Sas-4
CPAP
Sas-6
Daughter Centriole
Mother
Daughter Scaffold
Ana1
CEP295
Polo
PLK1
Spd-2
CEP192
Polo
AurA
Cnn
CDK5RAP2
TACC
PCM
Mother
PCM Scaffold
C
1µm magnetic streptavidin bead
Biotinylated Nanobodies (anti-GFP)
Nanobody-coated beads
Beads injection
Drosophila early embryos
(GFP-fusion of interest Jup-mCh)
centrosomes internal
GFP-bound beads
Pull beads to cortex with magnet
centrosomes arrive at cortex: compare behaviour of centrosomes and GFP-beads
D
Control beads
αGFP-Nb beads
Sas-6-GFP Ana2-GFP
MTs (Jup-mCh)
Merge
E
2.2% (91)
28.1% (601) (n)
GFP intensity (A.U.)
MTs+
MTs-
MT Intensity (A.U.)
Control beads
αGFP-Nb beads
F
Sas-6-GFP +Ana2-GFP
Sas-4
Merge
Sas-6-GFP +Ana2-GFP
Cnn
Merge
Asl
TACC
Spd-2
MTs
G
Sas-6/Ana2-beads
Centrosomes
Spd-2
Spd-2-mCh Intensity (A.U.)
Time (min)

Figure 1

Recapitulating centrosome assembly on synthetic beads. **(A)** Illustration of canonical centrosome duplication. **(B)** A proposed pathway of daughter centriole and mitotic PCM assembly in *Drosophila* embryos. These fly proteins all have human homologues whose names, if different, are indicated below the fly protein. **(C)** Illustration of the synthetic-bead injection assay. **(D)** Images show standard-resolution confocal images of uncoupled (control) or anti-GFP-Nanobody-coupled beads ~20-30mins after injection into an embryo expressing Sas-6-GFP, Ana2-GFP (*green*) and Jup-mCh (*magenta*, a marker of MTs). Control beads exhibit weak autofluorescence allowing them to be visualised (*arrows*). **(E)** Graphs quantify the intensity of GFP (top) or MTs (bottom) on individual beads, which were identified and measured computationally: beads above a threshold MT-fluorescence were scored as MT +ve (*brown dots*), beads below this threshold as MT -ve (*grey dots*) (see Figure S1 for methodology). The percentage of beads organising MTs (%) and the number of beads analysed (n) is indicated; N=5-15 embryos per condition. **(F)** Images show super-resolution confocal images of individual beads ~20-30min after injection into embryos expressing Sas-6-GFP, Ana2-GFP (*green*) and individual red-fluorescent fusions to various centriole/centrosome proteins (*magenta*). **(G)** Graph quantifies the fluorescence intensity (mean±SD) of the PCM-scaffold protein Spd-2-mCh at centrosomes (*orange squares*) and at Sas-6/Ana2-beads (*green dots*) int a typical embryo proceeding through nuclear cycle 11 and 12 (*pink shading* indicates mitosis). Scale bars = 5 μm.

Figure 2

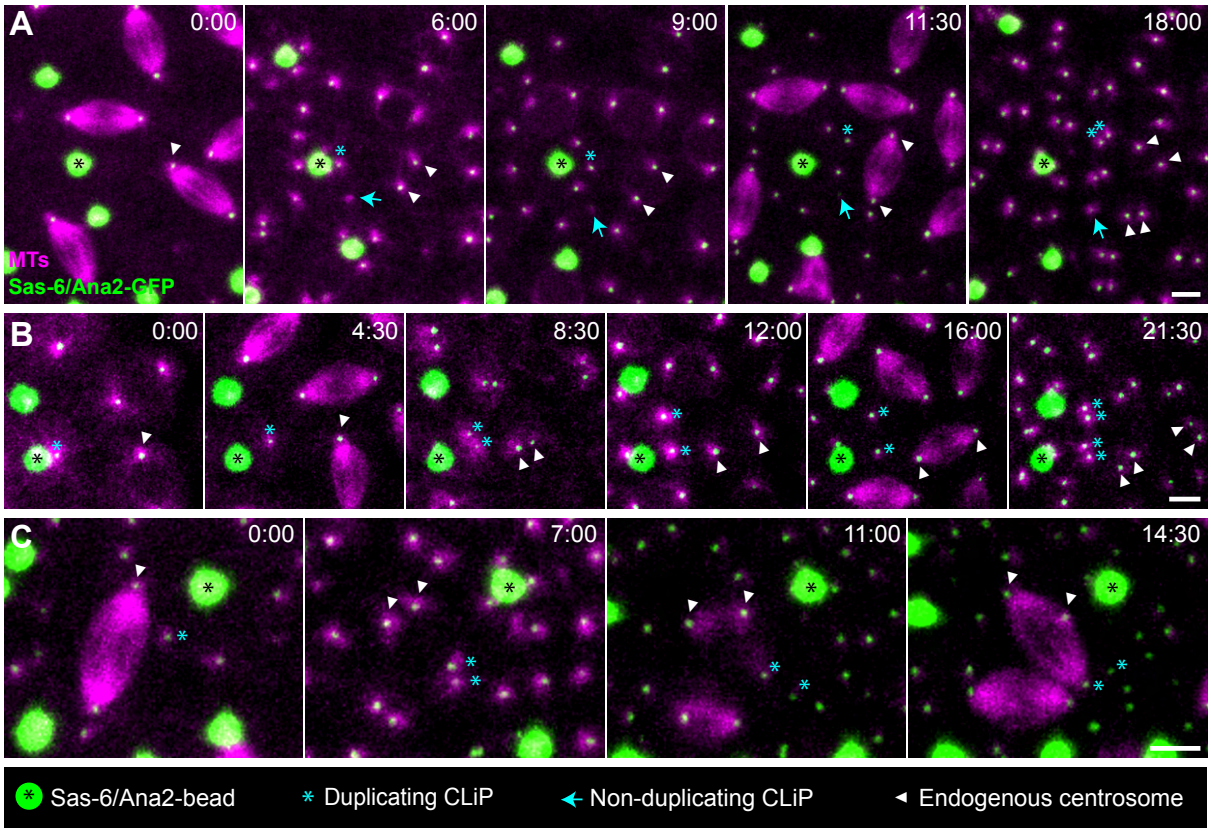

Figure 2

Sas-6/Ana2-beads generate **C**entrosome-**Li**ke **P**article**s** (**CLiPs**). Panels show stills from Movies of embryos expressing Sas-6-GFP, Ana2-GFP (*green*) and Jup-mCh (MTs) (*magenta*) injected with anti-GFP-Nanobody beads. Time (mins:secs) is indicated relative to the first image shown (t=0:00). Some beads (*black asterisks)*, CLiPs (*cyan asterisks* or *arrows)* and endogenous centrosomes (*white arrowheads*) are highlighted. **(A)** After mitosis (**t=0:00**) the highlighted bead generates six CLiPs (**t=6:00-9:00**) (see Movie S1), one of which is highlighted (*cyan asterisk*). All these CLiPs duplicate and then separate in synchrony with the endogenous centrosomes after the next round of mitosis (**t=11:30-18:00**). One CLiP (*cyan arrow*) generated by the bead below the highlighted bead is initially dimmer than the others and does not duplicate (Movie S1). **(B)** The highlighted bead generates a single CLiP that proceeds through two rounds of duplication in synchrony with the endogenous centrosomes (Movie S2). **(C)** The highlighted CLiP duplicates in synchrony with the endogenous centrosomes (**t=7:00**) and one "daughter" CLiP then displaces an endogenous centrosome to form a pole of a mitotic spindle during the next round of mitosis (**t=14:30**) (Movie S3). Scale bars = 5 µm.

Figure 3

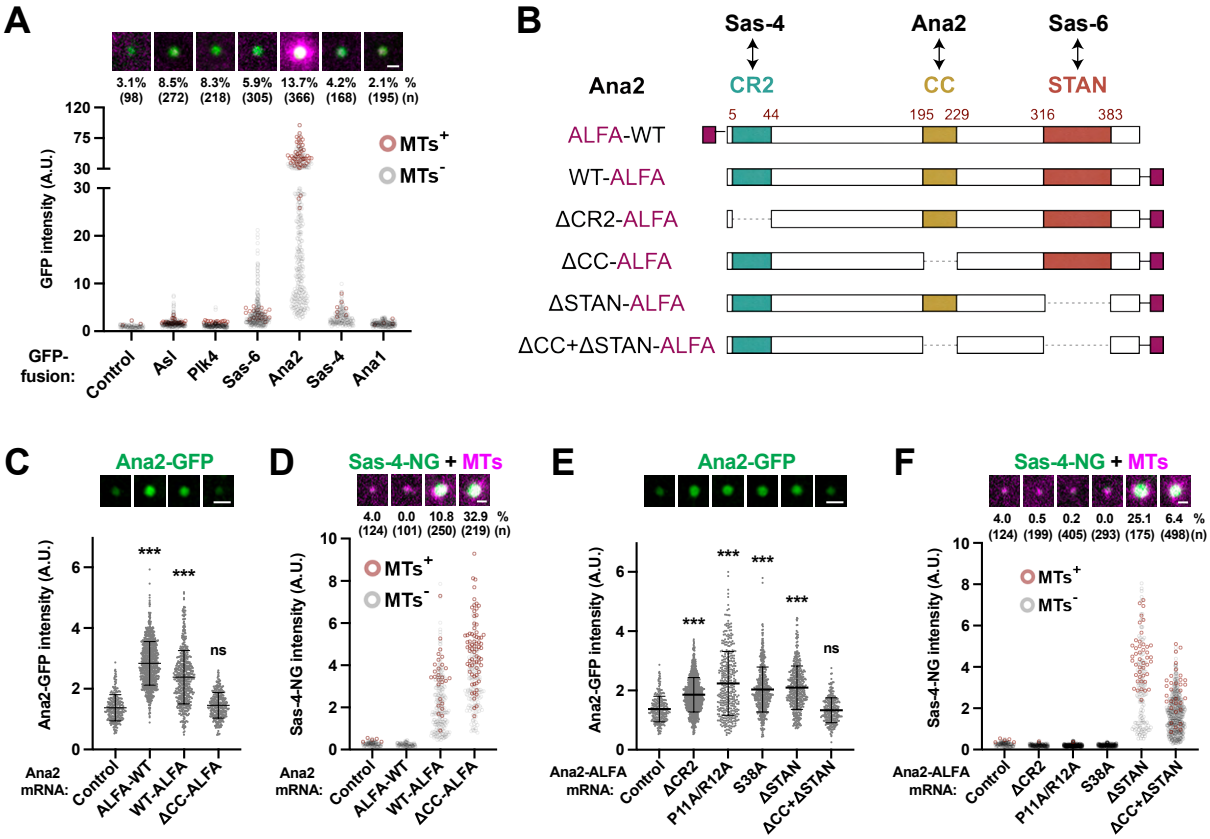

Figure 3

<u>Ana2 recruits Sas-4 to generate MTs and CLiPs.</u> **(A)** GFP-Nanobody beads were injected into embryos expressing various GFP-fusions (*green*) from their endogenous promoters and Jup-mCh (MT marker, *magenta*). Images show a representative bead, graph quantifies GFP-fusion intensity and indicate whether the beads organised MTs (*brown dots*) or not (*grey dots*). **(B)** Schematic illustration of the interaction domains of Ana2 and the ALFA-tagged (*purple box*) Ana2 constructs tested here. **(C)** Images show a representative bead and graph quantifies the recruitment of Ana2-GFP to various Ana2-ALFA-beads. **(D)** Images show a representative bead and graph quantifies the recruitment of Sas-4-NG and MTs to various Ana2-ALFA-beads. Note that the N-terminal ALFA-tag in ALFA-WT-Ana2 seems to strongly perturb the interaction with Sas-4, and so the ability of the beads to generate MTs/CLiPs. **(E,F)** Images show a representative bead and graphs quantify the recruitment of Ana2-GFP (E) or Sas-4-NG and Jup-mCh (F) to various WT and mutant Ana2-ALFA-beads. In all graphs, the percentage of beads organising MTs (%) and the number of beads analysed (n) is indicated; N=5-15 embryos per condition. Statistical analyses compare control to experimental beads and were performed using a one-way ANOVA in GraphPad Prism (ns=not significant; *** = $p<0.05$). Scale bars = 2 µm. Note that in this and subsequent Figures we did not statistically analyse experiments where we distinguish beads that are +/- MTs (see Materials and Methods for rationale). We found this was not required to appreciate biologically significant differences between experimental and control beads.

Figure 4

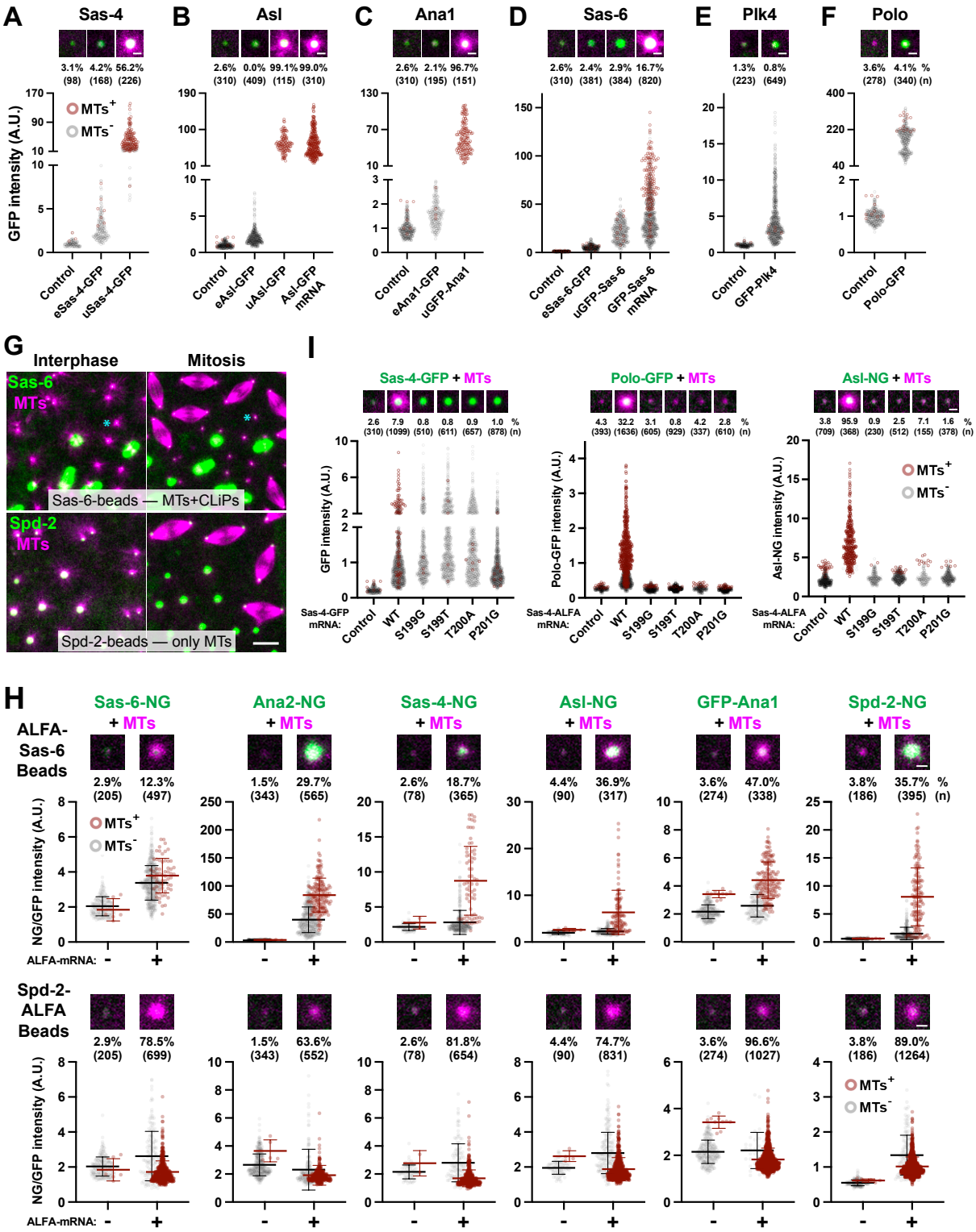
A
Sas-4
3.1% 4.2% 56.2%
(98) (168) (226)
GFP intensity (A.U.)
MTs+
MTs-
Control
eSas-4-GFP
uSas-4-GFP
B
Asl
2.6% 0.0% 99.1% 99.0%
(310) (409) (115) (310)
Control
eAsl-GFP
uAsl-GFP
Asl-GFP mRNA
C
Ana1
2.6% 2.1% 96.7%
(310) (195) (151)
Control
eAna1-GFP
uGFP-Ana1
D
Sas-6
2.6% 2.4% 2.9% 16.7%
(310) (381) (384) (820)
Control
eSas-6-GFP
uGFP-Sas-6
GFP-Sas-6 mRNA
E
Plk4
1.3% 0.8%
(223) (649)
Control
GFP-Plk4
F
Polo
3.6% 4.1% %
(278) (340) (n)
Control
Polo-GFP
G
Interphase
Mitosis
Sas-6
MTs
Sas-6-beads — MTs+CLiPs
Spd-2
MTs
Spd-2-beads — only MTs
I
Sas-4-GFP + MTs
2.6 7.9 0.8 0.8 0.9 1.0 %
(310) (1099) (510) (611) (657) (878) (n)
GFP intensity (A.U.)
Sas-4-GFP mRNA:
Control
WT
S199G
S199T
T200A
P201G
Polo-GFP + MTs
4.3 32.2 3.1 0.8 4.2 2.8 %
(393) (1636) (605) (929) (337) (610) (n)
Polo-GFP intensity (A.U.)
Sas-4-ALFA mRNA:
Asl-NG + MTs
3.8 95.9 0.9 2.5 7.1 1.6 %
(709) (368) (230) (512) (155) (378) (n)
Asl-NG intensity (A.U.)
Sas-4-ALFA mRNA:
H
ALFA-Sas-6 Beads
Sas-6-NG + MTs
2.9% 12.3%
(205) (497)
Ana2-NG + MTs
1.5% 29.7%
(343) (565)
Sas-4-NG + MTs
2.6% 18.7%
(78) (365)
Asl-NG + MTs
4.4% 36.9%
(90) (317)
GFP-Ana1 + MTs
3.6% 47.0%
(274) (338)
Spd-2-NG + MTs
3.8% 35.7% %
(186) (395) (n)
NG/GFP intensity (A.U.)
ALFA-mRNA: - +
Spd-2-ALFA Beads
2.9% 78.5%
(205) (699)
1.5% 63.6%
(343) (552)
2.6% 81.8%
(78) (654)
4.4% 74.7%
(90) (831)
3.6% 96.6%
(274) (1027)
3.8% 89.0%
(186) (1264)

Figure 4

Beads coupled to several individual centriole assembly proteins can generate CLiPs using the canonical centriole-assembly pathway. **(A-F)** Images show a representative bead and graphs quantify the recruitment of Jup-mCh (MT marker, *magenta*) and various GFP-fusions (*green*) to anti-GFP-Nanobody coupled beads injected into embryos expressing different levels of each GFP-fusion protein. The endogenous promotor (e), ubiquitin promoter (u) and mRNA injection generate embryos with progressively increasing levels of protein expression. Note that the overexpression of GFP-Plk4 or Polo-GFP could not be tested in these embryos due to lethality but, at the expression levels tested, both proteins did not generate MTs or CLiPs even though they were recruited to beads well above background levels. **(G)** Images show stills from Movies comparing Sas-6-beads (*top panels*) and Spd-2-beads (*bottom panels*) (*green*) in interphase and mitosis: both beads can generate MTs, but only Sas-6-beads can generate CLiPs (e.g., *cyan* asterisk). **(H)** Images show a representative bead and graphs compare the ability of ALFA-Sas-6-beads and Spd-2-ALFA-beads to recruit various green-fluorescent fusions (*green*) and generate MTs. The mean±SD is indicated and, for ease of comparison, beads organising (*brown dots*)/not organising (*grey dots*) MTs are slightly offset on the graphs. (see Figure S4 for data on other key proteins coupled to beads) **(I)** Images show a representative bead and graphs quantify the recruitment of Jup-mCh (MTs) and either Sas-4-GFP, Polo-GFP or Asl-NG to beads coupled to WT Sas-4 or various mutant forms of Sas-4. In all graphs the percentage of beads organising MTs (%) and the number of beads analysed (n) is indicated; N=5-15 embryos per condition. Scale bars: (A-F,I,H) = 2 µm; (G) = 10 µm.

Figure 5

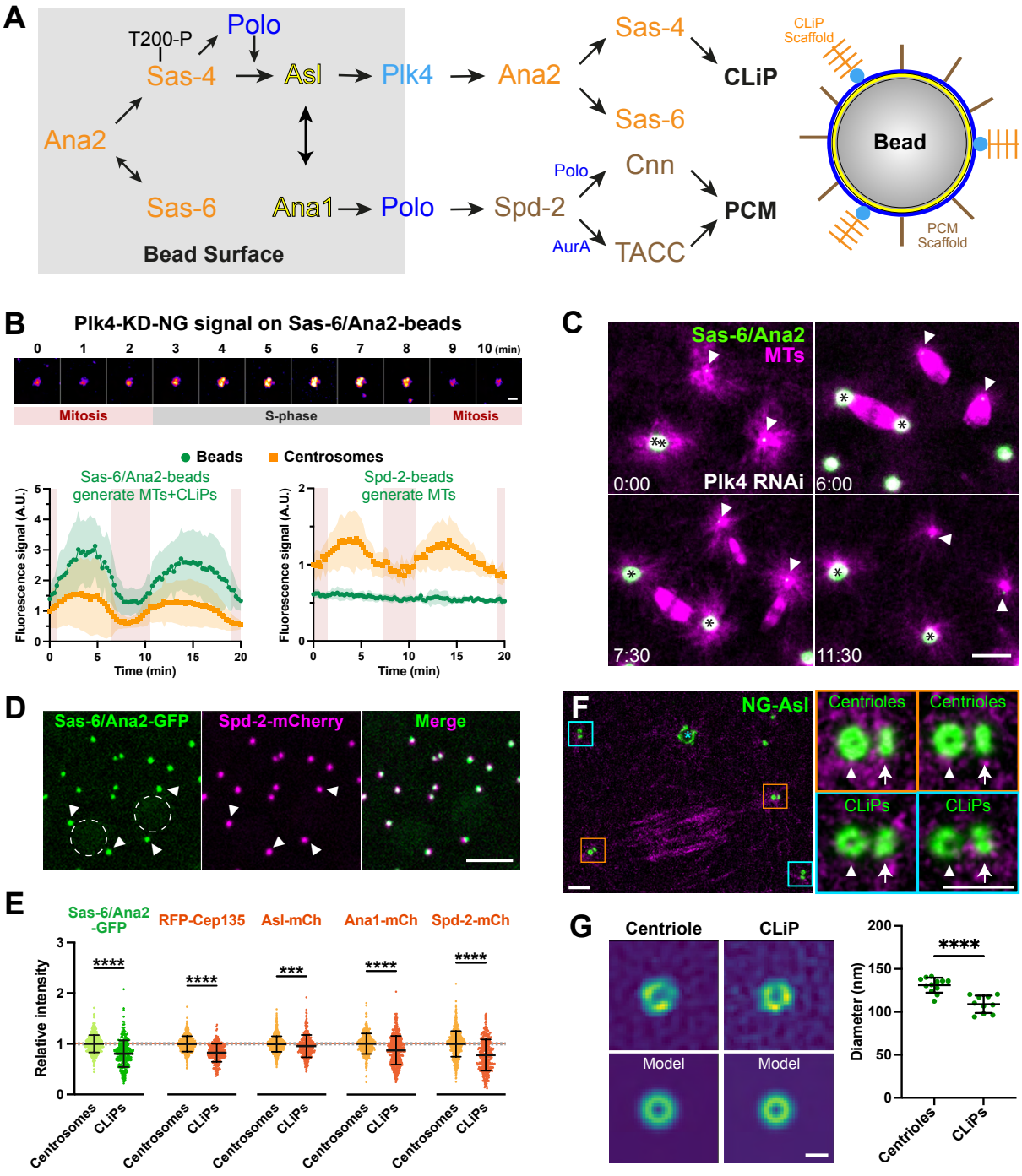
A
T200-P
Polo
Sas-4
Asl
Plk4
Ana2
Ana2
Sas-6
Ana1
Polo
Spd-2
Bead Surface
Sas-4
Sas-6
CLiP
Polo
Cnn
AurA
TACC
PCM
CLiP Scaffold
Bead
PCM Scaffold
B
Plk4-KD-NG signal on Sas-6/Ana2-beads
0 1 2 3 4 5 6 7 8 9 10 (min)
Mitosis
S-phase
Mitosis
Beads
Centrosomes
Sas-6/Ana2-beads generate MTs+CLiPs
Spd-2-beads generate MTs
Fluorescence signal (A.U.)
Time (min)
C
Sas-6/Ana2 MTs
Plk4 RNAi
0:00
6:00
7:30
11:30
D
Sas-6/Ana2-GFP
Spd-2-mCherry
Merge
E
Sas-6/Ana2 -GFP
RFP-Cep135
Asl-mCh
Ana1-mCh
Spd-2-mCh
Relative intensity
****
****
***
****
****
Centrosomes
CLiPs
F
NG-Asl
Centrioles
Centrioles
CLiPs
CLiPs
G
Centriole
CLiP
Model
Model
Diameter (nm)
****
Centrioles
CLiPs

Figure 5

Plk4 is required for beads to generate CLiPs, which appear to be molecularly and structurally similar to centrioles. **(A)** Schematic illustrates how the canonical centriole and PCM assembly pathways (see Fig.1B) may be co-opted by beads to generate CLiPs and PCM. If coupled to beads at a high enough concentration, any one of the core centriole assembly proteins (Ana2, Sas-6, Sas-4, Asl and Ana1) appears to initiate interactions with other core proteins that lead to the engagement of the canonical centriole/CLiP and PCM-assembly pathways at the bead surface. **(B)** Images illustrate and graphs quantify how Sas-6/Ana2-beads generate a pulse of kinase-dead Plk4 (Plk4-KD)-NG recruitment, in phase with the endogenous centrioles, during nuclear cycle 11-12 (mitosis indicated by *pink shading*). Spd-2-beads do not generate CLiPs and do not generate a pulse of Plk4-KD-NG recruitment. **(C)** Images from a Movie of Sas-6/Ana2-beads (*black asterisks*) in an embryo expressing Jup-mCh (MTs, *magenta*) injected with Plk4 RNAi. The centrosomes in these embryos stop duplicating so spindles have only one centrosome (*arrowheads*). These embryos proceed through cycles of S- and M-phase and the beads organise MTs that cycle in synchrony with the endogenous centrosomes, but the centrioles cannot duplicate and the beads cannot generate CLiPs. **(D,E)** Panels (D) illustrate and graphs (E) quantify the fluorescence intensity of various proteins at centrosomes (*arrowheads*) and CLiPs (*not labelled*). Images were analysed just prior to NEB so the weak nuclear fluorescence of Sas-6/Ana2-GFP (*dashed circles*) could be used to identify the endogenous centrosomes by their association with nuclei. (n=300-600 centrosomes/CLiPs analysed; N=5-15 embryos, per condition) **(F)** A super-resolution image (left) of NG-Asl in a living embryo showing the duplicated centrioles at the poles of a spindle (*orange boxes*) and two duplicated CLiPs in the cytoplasm (*cyan boxes*) that are all separating at the end of mitosis. A bead in the embryo that is generating 4 CLiPs is indicated (*cyan asterisk*). Magnified images (right) highlight the top-down barrel (*arrowhead*) or side-on bar (*arrow*) view of the Asl torus on the centrioles/CLiPs. Note that the magnified images have been rotated to align their orientations. **(G)** Panels show example images of the NG-Asl torus at an endogenous centriole (top left) and CLiP (top right) that were used to mathematically calculate the diameter of the underlying torus structure (Model). The graph shows the diameters of the modelled structures (n=12 centrioles and 10 CLiPs analysed). Statistical analyses (E,G) were performed using a Students t-test in GraphPad Prism (*** = $p<0.001$; **** = $p<0.001$). Scale bars: (B) = 2 µm; (C,D) = 10 µm; (F) = 1 µm; (G) = 200 nm.

References

1. W. F. Marshall, Scaling of Subcellular Structures. *Annual Review of Cell and Developmental Biology* **36**, 219–236 (2020).

2. S. Banerjee, W. A. Prinz, Early steps in the birth of four membrane-bound organelles—Peroxisomes, lipid droplets, lipoproteins, and autophagosomes. *Current Opinion in Cell Biology* **84**, 102210 (2023).

3. D. R. Kellogg, A growing problem: The many unsolved mysteries of cell growth. *MBoC* **36**, pe8 (2025).

4. W. F. Marshall, Cell Geometry: How Cells Count and Measure Size. *Annu Rev Biophys* **45**, 49–64 (2016).

5. D. K. Breslow, A. J. Holland, Mechanism and Regulation of Centriole and Cilium Biogenesis. *Annu. Rev. Biochem.* **88**, annurev-biochem-013118-111153 (2019).

6. A. Vasquez-Limeta, J. Loncarek, Human centrosome organization and function in interphase and mitosis. *Seminars in Cell & Developmental Biology* **117**, 30–41 (2021).

7. V. E. Foe, B. M. Alberts, Studies of nuclear and cytoplasmic behaviour during the five mitotic cycles that precede gastrulation in Drosophila embryogenesis. *J Cell Sci* **61**, 31–70 (1983).

8. P. T. Conduit, A. Wainman, J. W. Raff, Centrosome function and assembly in animal cells. *Nat Rev Mol Cell Biol* **16**, 611–624 (2015).

9. N. Banterle, P. Gönczy, Centriole Biogenesis: From Identifying the Characters to Understanding the Plot. *Annu Rev Cell Dev Biol* **33**, 23–49 (2017).

10. N. S. Dzhindzhev, G. Tzolovsky, Z. Lipinszki, S. Schneider, R. Lattao, J. Fu, J. Debski, M. Dadlez, D. M. Glover, Plk4 phosphorylates Ana2 to trigger Sas6 recruitment and procentriole formation. *Curr. Biol* **24**, 2526–2532 (2014).

11. M. Ohta, T. Ashikawa, Y. Nozaki, H. Kozuka-Hata, H. Goto, M. Inagaki, M. Oyama, D. Kitagawa, Direct interaction of Plk4 with STIL ensures formation of a single procentriole per parental centriole. *Nat Commun* **5**, 5267 (2014).

12. T. C. Moyer, K. M. Clutario, B. G. Lambrus, V. Daggubati, A. J. Holland, Binding of STIL to Plk4 activates kinase activity to promote centriole assembly. *J Cell Biol* **209**, 863–878 (2015).

13. A.-S. Kratz, F. Bärenz, K. T. Richter, I. Hoffmann, Plk4-dependent phosphorylation of STIL is required for centriole duplication. *Biology Open* **4**, 370–377 (2015).

14. N. S. Dzhindzhev, G. Tzolovsky, Z. Lipinszki, M. Abdelaziz, J. Debski, M. Dadlez, D. M. Glover, Two-step phosphorylation of Ana2 by Plk4 is required for the sequential loading of Ana2 and Sas6 to initiate procentriole formation. *Open Biol* **7**, 170247–11 (2017).

15. T. C. Moyer, A. J. Holland, PLK4 promotes centriole duplication by phosphorylating STIL to link the procentriole cartwheel to the microtubule wall. *eLife* **8**, 570 (2019).

16. P. T. Conduit, J. H. Richens, A. Wainman, J. Holder, C. C. Vicente, M. B. Pratt, C. I. Dix, Z. A. Novak, I. M. Dobbie, L. Schermelleh, J. W. Raff, A molecular mechanism of mitotic centrosome assembly in Drosophila. *Elife* **3**, e03399 (2014).

17. S.-S. Wong, J. M. Monteiro, C.-C. Chang, M. Peng, N. Mohamad, T. L. Steinacker, B. Xiao, S. Saurya, A. Wainman, J. W. Raff, Centrioles generate two scaffolds with distinct biophysical properties to build mitotic centrosomes. *Science Advances* **11**, eadq9549 (2025).

18. L. Gartenmann, C. C. Vicente, A. Wainman, Z. A. Novak, B. Sieber, J. H. Richens, J. W. Raff, Drosophila Sas-6, Ana2 and Sas-4 self-organise into macromolecular structures that can be used to probe centriole and centrosome assembly. *J Cell Sci* **133**, jcs244574 (2020).

19. S.-S. Wong, Z. M. Wilmott, S. Saurya, I. Alvarez-Rodrigo, F. Y. Zhou, K.-Y. Chau, A. Goriely, J. W. Raff, Centrioles generate a local pulse of Polo/PLK1 activity to initiate mitotic centrosome assembly. *EMBO J* **41**, e110891 (2022).

20. J. Huang, J. W. Raff, The disappearance of cyclin B at the end of mitosis is regulated spatially in Drosophila cells. *EMBO J* **18**, 2184–2195 (1999).

21. J. A. Farrell, P. H. O'Farrell, From egg to gastrula: how the cell cycle is remodeled during the Drosophila mid-blastula transition. *Annu Rev Genet* **48**, 269–294 (2014).

22. H. Götzke, M. Kilisch, M. Martínez-Carranza, S. Sograte-Idrissi, A. Rajavel, T. Schlichthaerle, N. Engels, R. Jungmann, P. Stenmark, F. Opazo, S. Frey, The ALFA-tag is a highly versatile tool for nanobody-based bioscience applications. *Nat Commun* **10**, 4403 (2019).

23. M. A. Cottee, N. Muschalik, S. Johnson, J. Leveson, J. W. Raff, S. M. Lea, The homo-oligomerisation of both Sas-6 and Ana2 is required for efficient centriole assembly in flies. *Elife* **4**, e07236 (2015).

24. M. A. Cottee, N. Muschalik, Y. L. Wong, C. M. Johnson, S. Johnson, A. Andreeva, K. Oegema, S. M. Lea, J. W. Raff, M. van Breugel, Crystal structures of the CPAP/STIL complex reveal its role in centriole assembly and human microcephaly. *Elife* **2**, e01071 (2013).

25. G. N. Hatzopoulos, M. C. Erat, E. Cutts, K. B. Rogala, L. M. Slater, P. J. Stansfeld, I. Vakonakis, Structural analysis of the G-box domain of the microcephaly protein CPAP suggests a role in centriole architecture. *Structure* **21**, 2069–2077 (2013).

26. Z. A. Novak, A. Wainman, L. Gartenmann, J. W. Raff, Cdk1 Phosphorylates Drosophila Sas-4 to Recruit Polo to Daughter Centrioles and Convert Them to Centrosomes. *Dev Cell* **37**, 545–557 (2016).

27. S. Yamamoto, D. Kitagawa, Emerging insights into symmetry breaking in centriole duplication: updated view on centriole duplication theory. *Current Opinion in Structural Biology* **66**, 8–14 (2021).

28. Z. M. Wilmott, A. Goriely, J. W. Raff, A simple Turing reaction–diffusion model explains how PLK4 breaks symmetry during centriole duplication and assembly. *PLOS Biology* **21**, e3002391 (2023).

29. M. G. Aydogan, T. L. Steinacker, M. Mofatteh, Z. M. Wilmott, F. Y. Zhou, L. Gartenmann, A. Wainman, S. Saurya, Z. A. Novak, S.-S. Wong, A. Goriely, M. A. Boemo, J. W. Raff, An Autonomous Oscillation Times and Executes Centriole Biogenesis. *Cell* **181**, 1566-1581.e27 (2020).

30. S. Yamamoto, D. Kitagawa, Self-organization of Plk4 regulates symmetry breaking in centriole duplication. *Nat Commun* **10**, 1810 (2019).

31. P. Scott, A. Curinha, C. Gliech, A. J. Holland, PLK4 self-phosphorylation drives the selection of a single site for procentriole assembly. *Journal of Cell Biology* **222**, e202301069 (2023).

32. C. Sullenberger, D. Kong, P. Avazpour, D. Luvsanjav, J. Loncarek, Centrosomal organization of Cep152 provides flexibility in Plk4 and procentriole positioning. *Journal of Cell Biology* **222**, e202301092 (2023).

33. J. Fu, D. M. Glover, Structured illumination of the interface between centriole and peri-centriolar material. *Open Biol* **2**, 120104 (2012).

34. V. Mennella, B. Keszthelyi, K. L. McDonald, B. Chhun, F. Kan, G. C. Rogers, B. Huang, D. A. Agard, Subdiffraction-resolution fluorescence microscopy reveals a domain of the centrosome critical for pericentriolar material organization. *Nat Cell Biol* **14**, 1159–1168 (2012).

35. M. H. Laporte, D. Gambarotto, É. Bertiaux, L. Bournonville, V. Louvel, J. M. Nunes, S. Borgers, V. Hamel, P. Guichard, Time-series reconstruction of the molecular architecture of human centriole assembly. *Cell*, doi: 10.1016/j.cell.2024.03.025 (2024).

36. K. K. Ito, K. Takumi, K. Matsuhashi, H. Sakamoto, K. Nagai, M. Fukuyama, S. Yamamoto, T. Chinen, S. Hata, D. Kitagawa, Multimodal mechanisms of human centriole engagement and disengagement. *The EMBO Journal*, 1–28 (2025).

37. D. J. Kushner, Self-assembly of biological structures. *Bacteriol Rev* **33**, 302–345 (1969).

38. J. J. McManus, P. Charbonneau, E. Zaccarelli, N. Asherie, The physics of protein self-assembly. *Current Opinion in Colloid & Interface Science* **22**, 73–79 (2016).

39. J. M. da C. Alves-Cruzeiro, R. Nogales-Cadenas, A. D. Pascual-Montano, CentrosomeDB: a new generation of the centrosomal proteins database for Human and Drosophila melanogaster. *Nucleic Acids Research* **42**, D430–D436 (2014).

40. I. Alvarez Rodrigo, T. L. Steinacker, S. Saurya, P. T. Conduit, J. Baumbach, Z. A. Novak, M. G. Aydogan, A. Wainman, J. W. Raff, Evidence that a positive feedback loop drives centrosome maturation in fly embryos. *Elife* **8** (2019).

41. I. Alvarez-Rodrigo, A. Wainman, S. Saurya, J. W. Raff, Ana1 helps recruit Polo to centrioles to promote mitotic PCM assembly and centriole elongation. *Journal of Cell Science* **134**, jcs258987 (2021).

42. D. Kong, V. Farmer, A. Shukla, J. James, R. Gruskin, S. Kiriyama, J. Loncarek, Centriole maturation requires regulated Plk1 activity during two consecutive cell cycles. *J Cell Biol* **206**, 855–865 (2014).

43. A. Shukla, D. Kong, M. Sharma, V. Magidson, J. Loncarek, Plk1 relieves centriole block to reduplication by promoting daughter centriole maturation. *Nat Commun* **6**, 8077 (2015).

44. G. Cabral, T. Laos, J. Dumont, A. Dammermann, Differential Requirements for Centrioles in Mitotic Centrosome Growth and Maintenance. *Dev Cell*, doi: 10.1016/j.devcel.2019.06.004 (2019).

45. J. Nunnari, P. Walter, Regulation of Organelle Biogenesis. *Cell* **84**, 389–394 (1996).

46. P. Yang, C. Mathieu, R.-M. Kolaitis, P. Zhang, J. Messing, U. Yurtsever, Z. Yang, J. Wu, Y. Li, Q. Pan, J. Yu, E. W. Martin, T. Mittag, H. J. Kim, J. P. Taylor, G3BP1 Is a Tunable Switch that Triggers Phase Separation to Assemble Stress Granules. *Cell* **181**, 325-345.e28 (2020).

47. G. B. Sissoko, E. V. Tarasovetc, O. Marescal, E. L. Grishchuk, I. M. Cheeseman, Higher-order protein assembly controls kinetochore formation. *Nat Cell Biol* **26**, 45–56 (2024).

48. G. K. Voeltz, E. M. Sawyer, G. Hajnóczky, W. A. Prinz, Making the connection: How membrane contact sites have changed our view of organelle biology. *Cell* **187**, 257–270 (2024).

49. M. Challiner, S. Saurya, S. Patel, J. W. Raff, M. Fostier, A. Prokop, Toward more sustainable research: reducing the environmental impact when working with Drosophila. *Genetics* **230**, iyaf114 (2025).

50. L. Gartenmann, A. Wainman, M. Qurashi, R. Kaufmann, S. Schubert, J. W. Raff, I. M. Dobbie, A combined 3D-SIM/SMLM approach allows centriole proteins to be localized with a precision of ~4-5 nm. *Curr. Biol.* **27**, R1054–R1055 (2017).

51. J.-Y. Tinevez, N. Perry, J. Schindelin, G. M. Hoopes, G. D. Reynolds, E. Laplantine, S. Y. Bednarek, S. L. Shorte, K. W. Eliceiri, TrackMate: An open and extensible platform for single-particle tracking. *Methods* **115**, 80–90 (2016).

52. M. G. Aydogan, A. Wainman, S. Saurya, T. L. Steinacker, A. Caballe, Z. A. Novak, J. Baumbach, N. Muschalik, J. W. Raff, A homeostatic clock sets daughter centriole size in flies. *J Cell Biol* **217**, 1233–1248 (2018).

53. Z. A. Novak, P. T. Conduit, A. Wainman, J. W. Raff, Asterless licenses daughter centrioles to duplicate for the first time in Drosophila embryos. *Curr. Biol.* **24**, 1276–1282 (2014).

54. S. Blachon, J. Gopalakrishnan, Y. Omori, A. Polyanovsky, A. Church, D. Nicastro, J. Malicki, T. Avidor-Reiss, Drosophila asterless and vertebrate Cep152 Are orthologs essential for centriole duplication. *Genetics* **180**, 2081–2094 (2008).

55. M. Buszczak, S. Paterno, D. Lighthouse, J. Bachman, J. Planck, S. Owen, A. D. Skora, T. G. Nystul, B. Ohlstein, A. Allen, J. E. Wilhelm, T. D. Murphy, R. W. Levis, E. Matunis, N. Srivali, R. A. Hoskins, A. C. Spradling, The Carnegie Protein Trap Library: A Versatile Tool for Drosophila Developmental Studies. *Genetics* **175**, 1505–1531 (2007).

56. T. L. Steinacker, S.-S. Wong, Z. A. Novak, S. Saurya, L. Gartenmann, E. J. H. van Houtum, J. R. Sayers, B. C. Lagerholm, J. W. Raff, Centriole growth is limited by the Cdk/Cyclin-dependent phosphorylation of Ana2/STIL. *Journal of Cell Biology* **221**, e202205058 (2022).

57. N. R. Stevens, J. Dobbelaere, K. Brunk, A. Franz, J. W. Raff, Drosophila Ana2 is a conserved centriole duplication factor. *J Cell Biol* **188**, 313–323 (2010).

58. N. Peel, N. R. Stevens, R. Basto, J. W. Raff, Overexpressing centriole-replication proteins in vivo induces centriole overduplication and de novo formation. *Curr Biol* **17**, 834–843 (2007).

59. C. I. Dix, J. W. Raff, Drosophila Spd-2 recruits PCM to the sperm centriole, but is dispensable for centriole duplication. *Curr Biol* **17**, 1759–1764 (2007).

60. S.-S. Wong, A. Wainman, S. Saurya, J. W. Raff, Regulation of centrosome size by the cell-cycle oscillator in Drosophila embryos. *The EMBO Journal* **43**, 414–436 (2024).

61. H. Roque, A. Wainman, J. Richens, K. Kozyrska, A. Franz, J. W. Raff, Drosophila Cep135/Bld10 maintains proper centriole structure but is dispensable for cartwheel formation. *J Cell Sci* **125**, 5881–5886 (2012).

62. P. T. Conduit, A. Wainman, Z. A. Novak, T. T. Weil, J. W. Raff, Re-examining the role of Drosophila Sas-4 in centrosome assembly using two-colour-3D-SIM FRAP. *Elife* **4**, 1032 (2015).

63. N. Karpova, Y. Bobinnec, S. Fouix, P. Huitorel, A. Debec, Jupiter, a new Drosophila protein associated with microtubules. *Cell Motility* **63**, 301–312 (2006).

64. A. Royou, C. Field, J. C. Sisson, W. Sullivan, R. Karess, Reassessing the Role and Dynamics of Nonmuscle Myosin II during Furrow Formation in Early Drosophila Embryos. *MBoC* **15**, 838–850 (2004).

Supplementary Material:

Materials and Methods

Fly stocks and husbandry

All *Drosophila* stocks used in this study are listed in Table S1. Flies were maintained at 18°C or 25°C in plastic vials or bottles on standard cornmeal-based medium. The food contained 0.68% agar, 2.5% yeast, 6.25% cornmeal, 3.75% molasses and preservatives (0.42% propionic acid, 0.7% ethanol and 0.14% tegosept). For embryo collection, adult flies were transferred to cages with fruit juice agar plates (40% cranberry-raspberry juice, 2% sucrose and 1.8% agar) supplemented with a drop of yeast paste. All fly work was performed using methods to minimise plastic waste and maximise environmental sustainability (*49*).

Synthetic beads preparation

Dynabeads MyOne Streptavidin C1 (65001, Invitrogen) were washed three times with PBS containing 0.01% Triton X-100 and 0.1% BSA (PBSTB), then incubated with biotinylated anti-GFP- or anti-ALFA-Nanobodies in PBSTB for at least 30 min at room temperature. Nanobody expression, biotinylation and purification were performed as previously described (*17*). The beads were then washed three times in PBSTB and stored at 3 mg/ml in PBSTB at 4 °C for up to one week.

Molecular constructs

cDNA fragments encoding Sas-6, Ana2, Sas-4, Asl and Plk4 were amplified from *Drosophila* cDNA as inserts, and pRNA plasmids containing GFP, ALFA or NG tags were amplified as vectors using Phusion™ Flash High-Fidelity PCR Master Mix (F548, Thermo Fisher Scientific). Following amplification, DpnI (R0176, NEB) was added to each reaction and incubated at 37 °C for 1 h, and PCR products were subsequently purified using QIAquick PCR Purification Kit (28106, QIAGEN). Fragments were then assembled using NEBuilder HiFi DNA Assembly Master Mix (E5520, NEB) and incubated at 50 °C for 30 min. Deletion constructs lacking specific domains or containing various point mutations were generated using the same method.

For Plk4 RNA interference (RNAi), primer pairs were designed in MacVector to target a 600 nt region of the Plk4 cDNA and were checked for potential off-target effects using NCBI-BLAST. The target region was amplified from Plk4 cDNA using Phusion™ Flash High-Fidelity PCR Master Mix. After purification with the QIAquick PCR Purification Kit, a T7 RNA polymerase promoter sequence was added to the fragments using a universal primer. The resulting PCR products were purified once more as described above.

All primer sequences used in this study are listed in Table S2.

In vitro transcription

Plasmid constructs for mRNA preparation were digested and linearised with AscI (R0558, NEB), followed by purification using the QIAquick PCR Purification Kit (28106, QIAGEN). The linearised DNA was then used for *in vitro* transcription with the mMESSAGE mMACHINE™ T3 Transcription Kit (AM1348, Thermo Fisher Scientific). The resulting mRNA was purified using the RNeasy MinElute Cleanup Kit (74204, Qiagen) and stored at -70 °C. All plasmids used in this study are listed in Table S3.

For Plk4 short interfering RNA (siRNA) preparation, the PCR product was transcribed using the MEGAscript™ T7 transcription Kit (AM1334, Invitrogen). The

transcripts were then precipitated by adding 10% volume of 3M sodium acetate and 2.5 volumes of ethanol, then incubated on ice for 5 min. After centrifugation at 4 °C for 10 min at full speed, the pellet was washed twice with cold 70% ethanol and dissolved in RNase-free water. The synthesised single-stranded RNAs were then annealed by incubation at 67.5 °C for 30 min, followed by slow cooling to room temperature over 60 min. The resulting double-stranded RNA was purified as described above and stored at -70 °C.

Embryo collection and injection

Embryos were collected from fruit juice agar plates after a 30-min egg-laying period at 25°C. Embryos were manually dechorionated and mounted on a strip of glue on 35-mm glass-bottom dishes with 14-mm microwells (P35G-1.5-14-C, MatTek). Mounted embryos were desiccated for 5 min at 25°C, then covered with Voltalef oil (H10S PCTFE, Arkema). Nanobody-coated beads were mixed with mRNA or water to a final concentration of 1 mg/ml (beads), 150 ng/ml (mRNA) and 100 ng/ml (siRNA). Embryos were injected with the bead mixture and incubated for an additional 30 min at 25°C prior to imaging. This last incubation was performed on a magnet to pull the injected beads to the embryo cortex for ease of imaging.

Spinning disk confocal microscopy

Embryos were imaged at room temperature using an Andor Dragonfly 505 spinning-disk confocal microscope (40-µm pinhole) mounted on a Leica DMi8 stand and controlled with Fusion software (Oxford Instruments). Excitation was provided by 488-nm and 561-nm solid-state diode lasers, and images were acquired with a HC PL APO 63×/1.40 NA oil-immersion objective and an Andor iXon Ultra 888 EMCCD camera. Z-stacks were collected over a stack of 41 optical sections with 0.5-µm z-spacing.

Super-resolution spinning disk confocal microscopy

Super-resolution microscopy was performed using a Nikon Eclipse Ti2 inverted microscope equipped with a SoRa super-resolution spinning-disk confocal unit (Yokogawa) and a high-sensitivity sCMOS camera. Imaging was carried out using a 60×/1.3 NA silicone immersion objective with silicone oil of refractive index 1.406 to minimise spherical aberration. The effective magnification was 240×, corresponding to a calibrated pixel size of 0.03 µm per pixel. Samples were excited using 488-nm and 561-nm laser lines, and fluorescence emission was collected using appropriate band-pass emission filters in combination with a quad-band dichroic mirror. Z-stacks were acquired over a total range of 6 µm with a z-step size of 0.3 µm.

Measurement of Asl torus radius

The radial localisation of the Asl was assessed as previously described (*50*) using a custom Python script (available at https://github.com/RaffLab/SIMcentriole-ring-measurement). Briefly, 10-15 Asl torus structures were selected and fitted with an elliptical annular Gaussian profile to determine the major and minor axis parameters. Toruses with low ring eccentricity, defined as a major-to-minor axis ratio of less than 1.2, were considered well oriented. The torus diameter was calculated as the average of the major and minor axes.

Image processing and analysis

Image stacks were processed in Fiji (ImageJ2, ver. 2.3.0/1.53q). Z-stacks were converted to maximum-intensity projections and corrected for photobleaching using the exponential fit algorithm. Background signal was subtracted using a rolling ball radius of 50 pixels. Beads were automatically detected and their fluorescence intensities quantified with the TrackMate plugin (*51*) using an estimated bead diameter of 3 µm.

SoRa super-resolution image reconstruction and 3D deconvolution were performed using NIS-Elements software (Nikon). Images were reconstructed using the SoRa mode (CSU W1-SoRa modality) and subsequently subjected to fast 3D deconvolution using the Richardson–Lucy MaxIP algorithm with medium noise settings for 8 iterations.

Fluorescence intensity measurements and statistical analyses were performed in GraphPad Prism, with details of the statistical tests provided in the corresponding figure legends.

Supplementary Figures

Fig. S1.

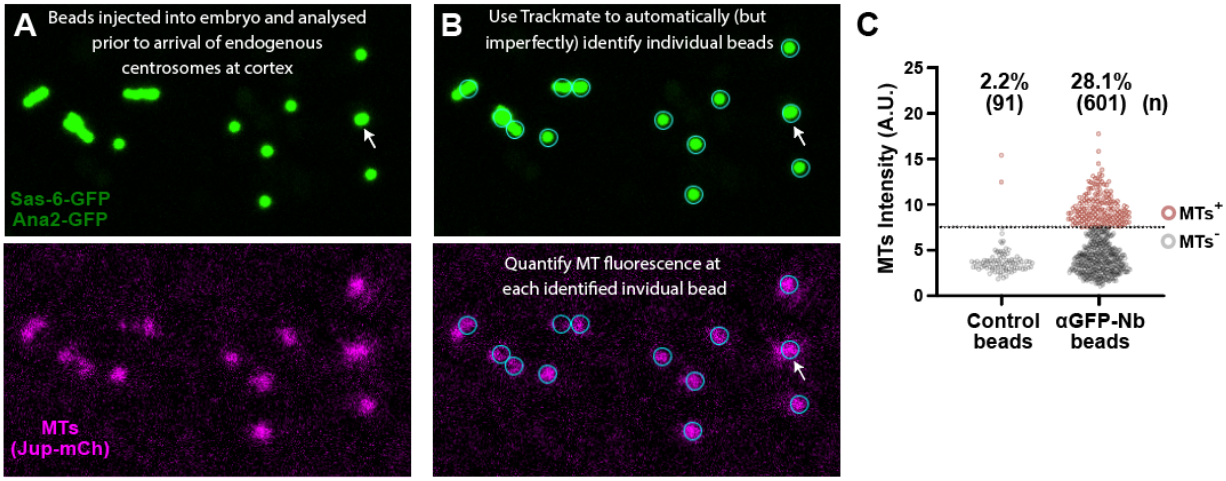

<u>Computational methodology for quantifying bead behaviour in embryos</u> **(A)** Panels show an embryo expressing Sas-6-GFP and Ana2-GFP (*green*, top panel) and Jup-mCherry (MT marker, *magenta*, bottom panel) that has been injected with anti-GFP-Nanobody-coupled beads. The beads in the embryo recruit the GFP-protein, but only some of them organise MTs efficiently. Often, there is a region in the embryo (right side of image) where the beads organise MTs efficiently and the beads are spread out (as the MTs tend to push the beads apart), and another region (left side of image) where the beads tend to clump together and only some of the beads organise MTs. It is difficult to assess how many beads are in each clump and how many of them organise MTs (see also Movie S5). **(B)** To quantify this type of data in an unbiased way we used the Fiji plug-in Trackmate to detect individual beads based on their GFP-fluorescence intensity (*cyan circles*) or, for controls where the beads did not organise MTs, on the weak red-autofluorescence of the beads (see Fig. 1D). This methodology is not very accurate at identifying individual beads within the clumps, but this does not significantly alter our conclusions (see below). The green- and red-fluorescence levels at each detected bead was then measured. For each experiment we compared the MT fluorescence levels of experimental beads to control beads injected into embryos of the same genotype. **(C)** This graph (also shown in Fig.1E) illustrates how after measuring the control and experimental beads we set a cutoff for MT intensity (*black dotted line*) at two standard-deviations above the mean intensity of the control beads. Any beads above this cutoff were scored as MT +ve (*brown dots*), and any beads below this cutoff as MT -ve (*grey dots*). The percentage of beads organising MTs (%) and the number of beads analysed (n) is indicated in each graph, and in all the experiments we report here N=5-15 embryos were scored per condition. While this methodology usually underestimates the number of beads in each clump and occasionally scores two or more closely spaced beads as one (*arrow*), it generated a graphical summary of the data that seemed to accurately convey the broad behaviour of each set of experimental beads relative to their controls.

Fig. S2.

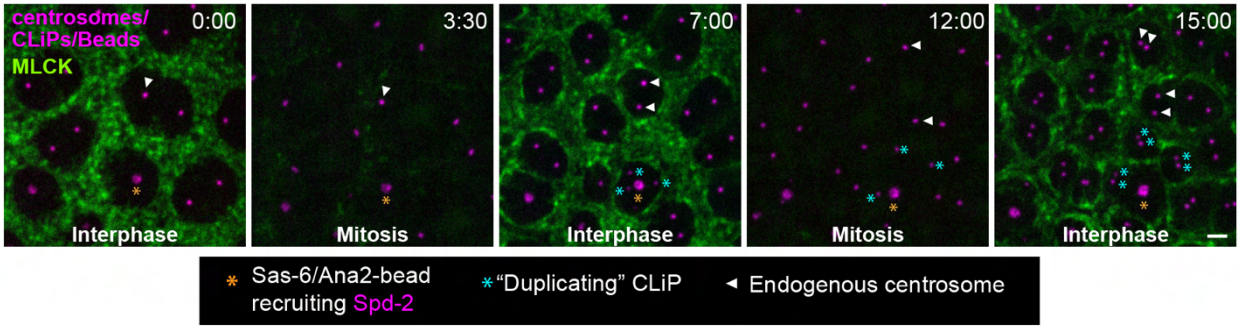

Like centrosomes, beads and CLiPs can organise cortical actomyosin. Panels show stills from a Movie (Movie S4) of an embryo expressing Myosin light-chain Kinase-GFP (MLCK-GFP) (*green*) and Spd-2-mCherry (as a marker of Beads/centrosomes/CLiPs, *magenta*) that was injected with beads coupled to an anti-ALFA-tag-Nanobody and mRNA encoding ALFA-tagged Ana2-ALFA and ALFA-Sas-6. As explained later in the main text, the ALFA-tag and anti-ALFA-tag-Nanobody can substitute for GFP and the anti-GFP-Nanobody in these bead experiments (Fig. 1C). The ALFA-tag is non-fluorescent, so in this experiment we monitor how the non-fluorescent Sas-6/Ana2-ALFA-beads recruit Spd-2-mCherry and organise MLCK-GFP in the embryo. At the start of the Movie (**t=0:00**; mins:secs) the embryo is in interphase and the endogenous centrosome pairs (one centrosome of a pair highlighted with an arrowhead) and their associated nuclei organise cortical MLCK-GFP around themselves (the cortical actomyosin that incorporates MLCK-GFP helps to keep each nucleus/centrosome pair separated from other nuclei/centrosomes in the common cytoplasm of the syncytial embryo). A single Sas-6/Ana2-bead is highlighted (*orange asterisk*), which also organised MLCK-GFP around itself. During mitosis the cortical actomyosin network incorporating MLCK-GFP disassembles (**t=3:30**) and then reassembles again at the end of mitosis (**t=7:00**), as the endogenous duplicated centrosomes separate. In this Movie, the Sas-6/Ana2-bead generates 4 CLiPs, 3 of which are highlighted (*cyan asterisks*). The CLiPs initially stay bounded within the cortical actomyosin network that surrounds the bead—just as the duplicated centrosomes stay bounded within the same actomyosin network around each nucleus (*arrowheads*). After another round of mitosis (t=12:00), the CLiPs have duplicated and separated, and each pair of CLiPs organises their own actomyosin network around themselves (**t=15:00**). Scale bar = 5 µm.

Fig. S3.

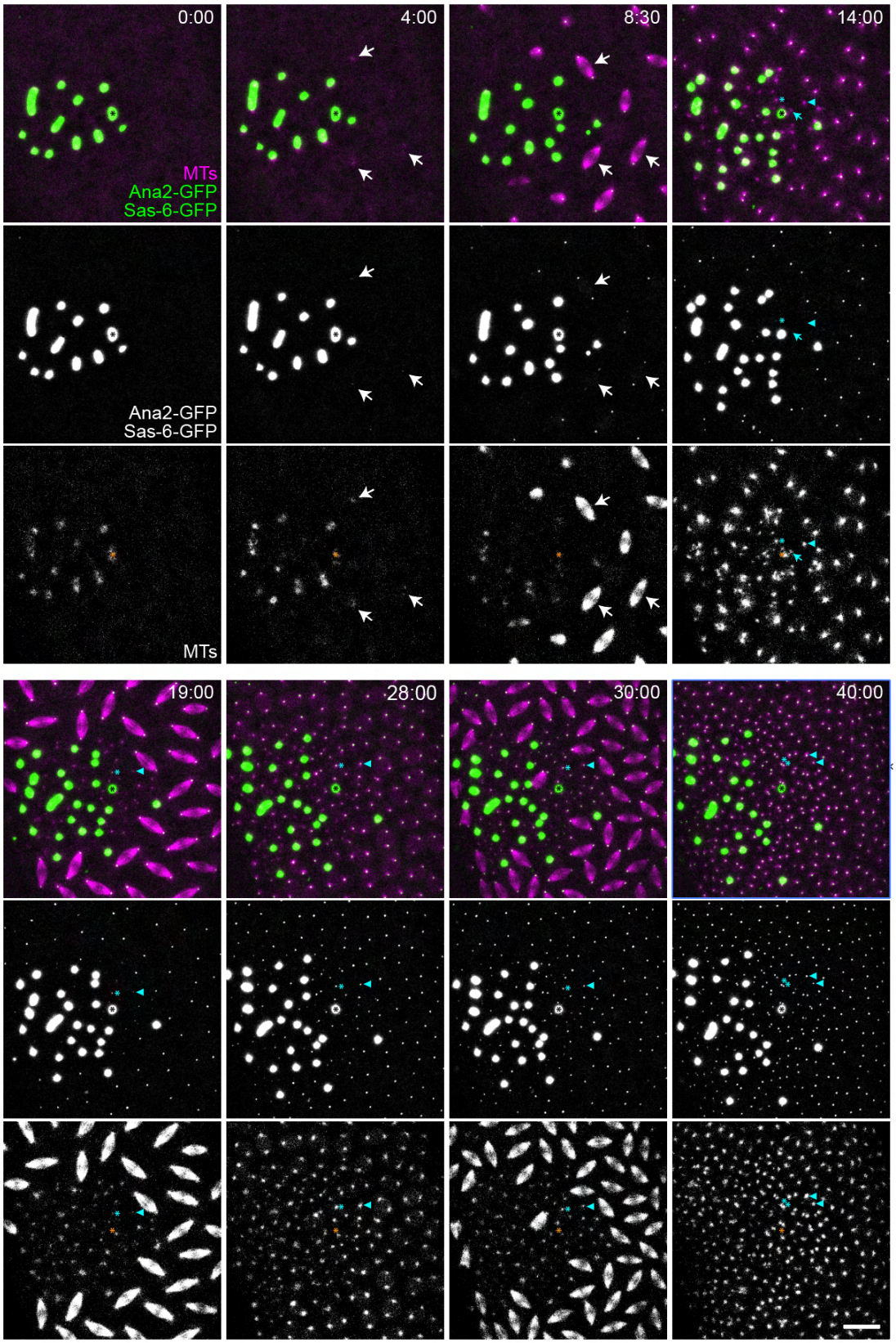
0:00
4:00
8:30
14:00
MTs
Ana2-GFP
Sas-6-GFP
Ana2-GFP
Sas-6-GFP
MTs
19:00
28:00
30:00
40:00

Sas-6/Ana2-beads can generate CLiPs when the endogenous centrosomes arrive at the cortex; some CLiPs dissipate while others mature and duplicate. Panels show stills from a Movie (Movie S5) of an embryo expressing Sas-6-GFP, Ana2-GFP (*green*) and Jup-mCh (MTs) (*magenta*) injected with anti-GFP-Nanobody beads. Time (mins:secs) is indicated and is relative to the first image shown (**t=0:00**), which was taken ~20-30mins after bead injection. At **t=0:00**, the endogenous nuclei and centrosomes have not yet migrated to the embryo cortex, and most of the injected beads (which have been pulled to the cortex by a magnet) are clumped together and have not generated any CLiPs. At **t=4:00**, the endogenous centrosomes start to arrive at the cortex (*white arrows*), and at **t=8:30** the embryo has entered mitosis. At **t=14:00** the embryo exits mitosis, and the endogenous duplicated centrosomes separate and move apart around their nuclei. At this stage, there is a burst of MT growth around the beads, which pushes several of the beads in clumps apart (compare beads at t=0:00 and t=14:00). At the same time, many of the beads generate several small Centrosome-Like Particles (CLiPs) that separate from the bead surface. Some of these CLiPs appear to be "immature" as they contain very low-levels of Sas-6/Ana2-GFP. Three CLiPs generated by the bead highlighted with the *black asterisk* (*orange asterisk* in the MT channel) are highlighted here (*cyan asterisk, arrow* or *arrowhead*). Sas-6/Ana2-GFP is initially detectable at the CLiP highlighted by the asterisk, but not at the CLiPs highlighted by the arrow or arrowhead. At **t=19:00** the embryo has entered the next round of mitosis: the CLiP highlighted by the *cyan arrow* has dissipated and is no longer detectable, but the CLiPs highlighted by the *cyan asterisk* and *arrowhead* have acquired more Sas-6/Ana2-GFP. These CLiPs do not appear to initially duplicate and so they do not separate into two after the embryo exits mitosis at **t=28:00**. Both CLiPs, however, acquire more Sas-6/Ana2-GFP during the next interphase and after the next round of mitosis (**t=30:00**) both CLiPs separate into two (**t=40:00**), indicating that they had duplicated in the previous interphase. This Movie illustrates how Sas-6/Ana2-beads do not generate CLiPs until the endogenous nuclei/centrosomes arrive at the embryo cortex, and how many CLiPs initially appear to be immature. Immature CLiPs can either dissipate or persist; if they persist, they acquire more Sas-6/Ana2 and can eventually duplicate and separate. It is not clear why some CLiPs initially appear to be immature, but we suspect that this is because the geometry of the bead is not optimised for Plk4 symmetry-breaking, so Plk4 may not be fully active at all the CLiP-generating sites on the bead-surface (discussed in more detail later in the manuscript). Scale bar = 10 μm.

Fig. S4.

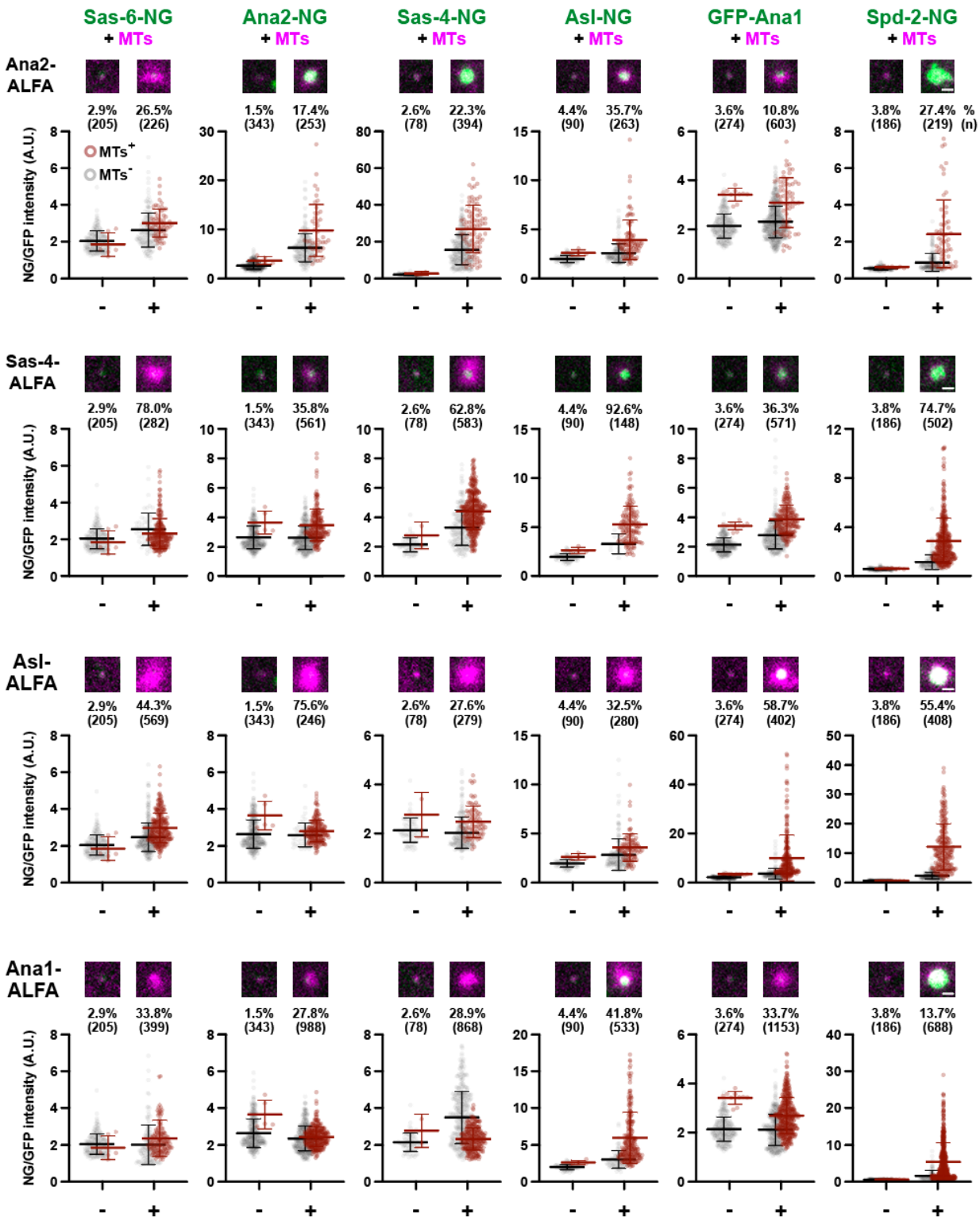
Sas-6-NG + MTs
Ana2-NG + MTs
Sas-4-NG + MTs
Asl-NG + MTs
GFP-Ana1 + MTs
Spd-2-NG + MTs
Ana2-ALFA
2.9% (205) 26.5% (226)
1.5% (343) 17.4% (253)
2.6% (78) 22.3% (394)
4.4% (90) 35.7% (263)
3.6% (274) 10.8% (603)
3.8% (186) 27.4% (219)
% (n)
MTs+
MTs-
NG/GFP intensity (A.U.)
Sas-4-ALFA
2.9% (205) 78.0% (282)
1.5% (343) 35.8% (561)
2.6% (78) 62.8% (583)
4.4% (90) 92.6% (148)
3.6% (274) 36.3% (571)
3.8% (186) 74.7% (502)
Asl-ALFA
2.9% (205) 44.3% (569)
1.5% (343) 75.6% (246)
2.6% (78) 27.6% (279)
4.4% (90) 32.5% (280)
3.6% (274) 58.7% (402)
3.8% (186) 55.4% (408)
Ana1-ALFA
2.9% (205) 33.8% (399)
1.5% (343) 27.8% (988)
2.6% (78) 28.9% (868)
4.4% (90) 41.8% (533)
3.6% (274) 33.7% (1153)
3.8% (186) 13.7% (688)
- +

Analysis of the ability of individual core centriole-assembly proteins to recruit other core proteins to beads to generate MTs and CLiPs. Images and graphs compare the ability of beads coupled to various ALFA-tagged fusions (indicated at top left of each panel) to recruit various green-fluorescent fusion proteins (*green*) and generate MTs (Jup-mCh, *magenta*). The percentage of beads organising MTs (%) and the number of beads analysed (n) is indicated in each graph; N=5-15 embryos for each condition. For ease of comparison, beads organising (*brown dots*)/not organising (*grey dots*) MTs are slightly offset on the graphs. Mean±SD is indicated for each dataset. This Figure is a continuation of Fig. 4H that showed the same analysis for Sas-6-ALFA-beads and Spd-2-ALFA-beads. This analysis broadly supports our conclusion that the pathways of canonical centriole-dependent centriole and PCM assembly (outlined in Fig.1B) are also used for bead-dependent CLiP and PCM assembly (outlined in Fig.5A). For example, when coupled to beads, Ana2 recruits relatively small amounts of Sas-6, but much more of itself and all the other core proteins, consistent with the data that Ana2 engages the rest of the pathway via Sas-4 recruitment without the need to recruit large amounts of Sas-6 (see Fig.3F). In contrast, Sas-6-beads that generate MTs/CLiPs recruit significant amounts of Ana2 (see Fig.4H), presumably because Sas-6-beads cannot engage the assembly pathways without recruiting Ana2 (see Fig.5A). Similarly, Sas-4 can engage the centriole and PCM assembly pathways without recruiting large amounts of Sas-6 or Ana2, while Asl and Ana1 can engage these pathways without recruiting large amounts of Sas-6, Ana2 or Sas-4—although Asl and Ana1 seem to need to recruit large amounts of each other, which is again consistent with the canonical pathway. All the core proteins recruit significant amounts of Spd-2 relative to controls, presumably explaining why all these beads can generate MTs. Note that all the core centriole assembly proteins should be recruited to beads at the site where any CLiP is assembling (as CLiPs contain all these proteins). This may explain why even beads that seem to recruit very little of a core protein (e.g. Sas-4-beads seem to recruit very little Sas-6 or Ana2) usually recruit at least slightly more of these proteins than controls—as some Sas-6 and Ana2 will be incorporating into the CLiPs being assembled on the bead surface. Scale bar = 2 μm.

Supplementary Tables

Table S1. Fly stocks used in this study.

Flies	Source	Figures	Movies
eSas-6-GFP	(*52*)	3A; 4D	
eAna2-GFP	(*52*)	3A,C,E	
ePlk4-GFP	(*52*)	3A	
eSas-4-GFP	(*53*)	3A; 4A	
eAsl-GFP	(*54*)	3A, 4B	
eAna1-GFP	(*54*)	3A; 4C	
Polo-GFP	(*55*)	4F,I	S11
eSas-6-GFP; eAna2-GFP	this study	1D-F; 2A-C; 5C-E; S1,3	S1-S3; S5; S12
eSas-4-NG	(*56*)	3D,F; 4H; S4	
eAsl-NG	(*56*)	4H,I; S4	
eNG-Asl	(*56*)	5F,G	S13
eSas-6-NG	(*56*)	4H; S4	
eAna2-NG	(*56*)	4H; S4	
Ubq-Asl-GFP	(*57*)	4B	S7
Ubq-Sas-4-GFP	(*58*)	4A,I	S6
Ubq-GFP-Ana1	(*41*)	4C,H; S4	S8
Ubq-GFP-Sas-6	(*58*)	4D	
Ubq-GFP-Plk4	(*58*)	4E	S10
Ubq-Spd-2-GFP	(*59*)	4G	
Ubq-Spd-2-NG	(*60*)	4H; S4	
Ubq-RFP-Cep135	(*61*)	5E	
Ubq-Asl-mCherry	(*62*)	5E	
Ubq-Spd-2-mCherry	(*40*)	1G; 5E; S2	
Ubq-Ana1-mCherry	(*41*)	5E	
Jupiter-mCherry	(*63*)	1D,E; 2; 3A,C-F; 4; 5C,F; S1; S3; S4	S1-S3; S5-S15
GFP-Sqh (Myosin regulatory light chain)	(*64*)	S2	S4

Table S2. Primers (5'-3') used in this study.

Plasmids	Inserts	Vectors
pRNA-GFP/ALFA-Sas-6	F: ACAAGTTTGTACAAAAAAGCAGGCTTCATGTGGCCTCCAGGGAGCGAGG R: CAACATATCCAGTCACTATGCTATCGCCGGTTTTCTTTGCCCGTG	F: TAGCATAGTGACTGGATATGTTGTGTTTTACAG R: GAAGCCTGCTTTTTTGTACAAACTTGTTGAAC
pRNA-ALFA-Ana2	F: ACAAGTTTGTACAAAAAAGCAGGCTTCATGTTTGTTCCCGAAACGG R: CAACATATCCAGTCACTATGCTACAACAGCTTCGGCTGGTTCC	
pRNA-Ana2-GFP/ALFA	F: CAGATCTGAATTCAGCCACCATATCAAATGTTTGTTCCCGAAACGG R: ACTTTGTACAAGAAAGCTGGGTCCAACAGCTTCGGCTGGTTCC	F: GACCCAGCTTTCTTGTACAAAGTGG R: TTGATATGGTGGCTGAATTCAGATC
pRNA-Asl-GFP/ALFA	F: GAATTCAGCCACCATATCAAATGAACACGCCAGGTATAAGC R: TTGTACAAGAAAGCTGGGTCGCTGTGACCATTGCCTTTGGG	
pRNA-Spd-2-ALFA	F: ACAAAAAAGCAGGCTTCATGGACAGTAG R: TTGTACAAGAAAGCTGGGTCAAATTTAAAACTAATCGG	
pRNA-Sas-4-GFP/ALFA	F: GAATTCAGCCACCATATCAAATGCAGGAGGCTGGCGAAAGTCC R: TTGTACAAGAAAGCTGGGTCATACTTGGCATAGTCTGTGTCC	
pRNA-Plk4-NG	F: ACAAGTTTGTACAAAAAAGCAGGCTTCATGTTATCCAATCGGGCGTTTG R: CAACATATCCAGTCACTATGCTAAAGAAGCATGCGATTATAATAAGGCG	
pRNA-Ana1-ALFA	F: ACAAAAAAGCAGGCTTCATGGCTCTG R: TTGTACAAGAAAGCTGGGTCTTTTCGGG	
Deletions/point mutations		
Ana2-ΔCC	F: CCCGAAGCCATTTCAAAAGC R: GCTTTTGAAATGGCTTCGGGCTTATTGGCCAAGTTGCTGAC	
Ana2-ΔSTAN	F: CCCGAGGAGCAACTGGAGCC R: GGCTCCAGTTGCTCCTCGGGGGTGTTGGGCTTGGCCAGTTG	

Ana2-ΔCR2	F: CATATCAAATGTTTGTTCCCCCGCAGGATCCGCAGATGCAG R: GGGAACAAACATTTGATATGGTGGCTGAATTC
Ana2-P11A/R12A	F: ACGGAGGATATGCTGGCCGCACTAGCGCCCAGGCCGAGTG R: GCGGCCAGCATATCCTCCGTTTCGGGAACAAAC
Ana2-S38A	F: CCGTGCCGGAGGTAGCCATATTGTTTGGCCAGCCG R: CAAACAATATGGCTACCTCCGGCACGGTGGGCCCTATAATCTC
Sas-4-S199G	F: TCGGCAAGAACGCCTGCAGTGGCACTCCAGATCTAAAGTCTTCCTATGC R: ACTGCAGGCGTTCTTGCCGATAAG
Sas-4-S199T	F: TCGGCAAGAACGCCTGCAGTACCACTCCAGATCTAAAGTCTTCCTATGC R: ACTGCAGGCGTTCTTGCCGATAAG
Sas-4-T200A	F: TCGGCAAGAACGCCTGCAGTTCCGCTCCAGATCTAAAGTCTTCCTATGC R: ACTGCAGGCGTTCTTGCCGATAAG
Sas-4-P201G	F: GCCTGCAGTTCCACTGGAGATCTAAAGTCTTCCTATGCGTCCTCCACAAC R: GATCTCCAGTGGAACTGCAGGCGTTCTTGCCGATAAG
Plk4-KD (D156A)	F: GATAGCCGCTTTTGGACTGGCCACCCAATTAAAG R: CCAGTCCAAAAGCGGCTATCTTGACGTGCATTTCCCTGC
RNAi	
Plk4 target region	F: AGACCACGGGCGGGTTTTCGGCCAACCTATAATGAAGATCG R: AGACCACGGGCGGGTTGGTGTGGAAAACGCAATATTGGTGG
Universal primer	TAATACGACTCACTATAGGGAGACCACGGGCGGGT

Table S3. Plasmids used for *in vitro* mRNA synthesis in this study.

Plasmids	Figures	Movies
pRNA-ALFA-Sas-6	1G; 4H; 5B,F,G; S2	S4; S13
pRNA-Ana2-ΔCC + ΔSTAN-ALFA	1G*; 3E,F; 5B,F,G*; S2*	S4*; S13*
	In these experiments, Ana2-ΔCC + ΔSTAN-ALFA mRNA was co-injected with ALFA-Sas-6 mRNA instead of WT Ana2 to avoid production of **Sas-6/**A**na2 **p**articles (**SAPs**).*	
pRNA-Ana2-GFP	3C,E	
pRNA-Ana2-ALFA	3C,D; S4	
pRNA-ALFA-Ana2	3C,D	
pRNA-Ana2-ΔCC-ALFA		
pRNA-Ana2-ΔCR2-ALFA	3E,F	
pRNA-Ana2-P11A/R12A-ALFA		
pRNA-Ana2-S38A-ALFA		
pRNA-Ana2-ΔSTAN-ALFA		
pRNA-Asl-GFP	4B	
pRNA-GFP-Sas-6	4D,G	S9
pRNA-Spd-2-ALFA	4H; 5B	
pRNA-Sas-4-GFP	4I	
pRNA-Sas-4-S199G-GFP		
pRNA-Sas-4-S199T-GFP		
pRNA-Sas-4-T200A-GFP		
pRNA-Sas-4-P201G-GFP		
pRNA-Sas-4-S199G-ALFA		
pRNA-Sas-4-S199T-ALFA		
pRNA-Sas-4-T200A-ALFA		
pRNA-Sas-4-P201G-ALFA		
pRNA-Sas-4-ALFA	4I; S4	
pRNA-Plk4-KD-NG	5B	
pRNA-Asl-ALFA	S4	
pRNA-Ana1-ALFA	S4	

Movies

Movie S1.
Sas-6/Ana2-beads generate CLiPs that can duplicate in synchrony with the endogenous centrosomes. Anti-GFP-Nanobody beads were injected into an embryo expressing Sas-6-GFP, Ana2-GFP (*green*) and Jup-mCh (MTs) (*magenta*). Time (mins:secs) is indicated and is relative to the first image (t=0:00), which was taken ~20-30mins after bead injection. A single Sas-6/Ana2-bead is highlighted (*black asterisk*) and this generates several CLiPs at the end of the first round of mitosis (one of which is highlighted (*cyan asterisk*); all these CLiPs duplicate in synchrony with the endogenous centrosomes after the next round of mitosis. A CLiP generated by the bead below the highlighted bead is also highlighted (*cyan arrow*). This CLiP is less bright than the others and it does not duplicate/separate at the end of the next round of mitosis. An endogenous centrosome is also highlighted (*white arrowheads*) that proceeds through two rounds of division. Note that after the second round of mitosis the highlighted Sas-6/Ana2-bead generates several more CLiPs, one of which is highlighted (*small yellow asterisk*).

Movie S2.
Sas-6/Ana2-beads generate CLiPs that can proceed through multiple rounds of duplication. Anti-GFP-Nanobody beads were injected into an embryo expressing Sas-6-GFP, Ana2-GFP (*green*) and Jup-mCh (MTs) (*magenta*). Time (mins:secs) is indicated and is relative to the first image (t=0:00), which was taken ~20-30mins after bead injection. The highlighted bead (*black asterisk*) generates a single CLiP that is highlighted (*cyan asterisk*); this proceeds through two rounds of duplication in synchrony with the endogenous centrosomes—one of which (and its progeny) are highlighted (*white arrowheads*).

Movie S3.
CLiPs can compete with centrosomes to form the poles of the mitotic spindle. Anti-GFP-Nanobody beads were injected into an embryo expressing Sas-6-GFP, Ana2-GFP (*green*) and Jup-mCh (MTs) (*magenta*). Time (mins:secs) is indicated and is relative to the first image (t=0:00), which was taken ~20-30mins after bead injection. A single CLiP (*cyan asterisk*) and endogenous centrosome (*white arrowhead*), and their progeny, are highlighted. The centrosome and CLiP both duplicate after the first round of mitosis generating two “daughter” centrosomes and two “daughter” CLiPs. During the second round of mitosis, one of the two daughter CLiPs displaces one of the daughter centrosomes from the pole of the forming mitotic spindle, so this spindle has one centrosome and one CLiP at its poles.

Movie S4.
Beads and CLiPs can organise cortical actomyosin structures. This Movie shows an embryo expressing Myosin light-chain Kinase-GFP (MLCK-GFP) (*green*) (as a marker of the cortical actomyosin) and Spd-2-mCherry (*magenta*) (as a marker of centrosomes, beads and CLiPs) that was injected with beads coupled to an anti-ALFA-

tag-Nanobody and mRNA encoding ALFA-tagged Ana2-ALFA and ALFA-Sas-6. As explained later in the main text, the ALFA-tag and anti-ALFA-tag-Nanobody can substitute for GFP and the anti-GFP-Nanobody, respectively, in these bead experiments. The ALFA-tag is non-fluorescent, so in this Movie we monitor how the centrosomes, beads and CLiPs (visualised with Spd-2-mCherry) can organise cortical actomyosin domains around themselves during interphase. Time (mins:secs) is indicated and is relative to the first image (t=0:00), which was taken ~20-30mins after bead injection. This Movie remains centred on a single bead within the embryo (*orange asterisk*), which generates 4 CLiPs after the first round of mitosis—3 of which are highlighted, *cyan asterisks*). These CLiPs initially remain within the same MLCK-domain as the bead but, after the next round of mitosis, all of the CLiPs duplicate and generate their own domain of MLCK-GFP around themselves (just as the endogenous centrosomes do—one of which is highlighted with a *white arrowhead*).

Movie S5.
Sas-6/Ana2-beads generate CLiPs only after the nuclei and centrosomes reach the embryo cortex, and some CLiPs appear to be immature. Anti-GFP-Nanobody beads were injected into an embryo expressing Sas-6-GFP, Ana2-GFP (*green*) and Jup-mCh (MTs) (*magenta*). Time (mins:secs) is indicated and is relative to the first image (t=0:00), which was taken ~20-30mins after bead injection. There are several typical behaviours of these beads that can be seen in this Movie: (1) Many of the beads are initially clumped together and gradually separate as the embryo develops and more of the beads organise MTs and generate CLiPs (compare the distribution of beads at the start and end of the Movie); (2) None of the beads initially generate CLiPs, but they start to do so after the first mitosis that occurs after the nuclei and centrosomes have arrived at the embryo cortex; (3) Many of the CLiPs generated do not immediately duplicate after the next round of mitosis, but do so after the embryo has proceeded through at least one additional round of mitosis (e.g. CLiPs highlighted with *cyan asterisk* and *arrowhead*). This suggests that some CLiPs are “immature” and are, at least initially, unable to duplicate.

Movie S6.
Beads bound to Sas-4-GFP can generate MTs and CLiPs. Anti-GFP-Nanobody beads were injected into an embryo expressing Sas-4-GFP (*green*) from the Ubq-promotor and Jup-mCh (MTs) (*magenta*). Time (mins:secs) is indicated and is relative to the first image (t=0:00), which was taken ~15-30mins after bead injection. The Sas-4-beads generate MTs and CLiPs. This Movie remains centred on a single bead (*black asterisk*) within the embryo, that generates 4 CLiPs after the first round of mitosis; 3 of these CLiPs duplicate after the next round of mitosis.

Movie S7.
Beads bound to Asl-GFP can generate MTs and CLiPs. Anti-GFP-Nanobody beads were injected into an embryo expressing Asl-GFP (*green*) from the Ubq-promotor and Jup-mCh (MTs) (*magenta*). Time (mins:secs) is indicated and is relative to the first

image (t=0:00), which was taken ~15-30mins after bead injection. For unknown reasons, the Asl-GFP-beads often remain clumped together, and this Movie is centred on a clump of beads (*black asterisk*) that at the start of the Movie have just generated multiple CLiPs. Most of these CLiPs duplicate after the next round of mitosis, when the clump of beads also generates another set of CLiPs.

Movie S8.
Beads bound to Ana1-GFP can generate MTs and CLiPs. Anti-GFP-Nanobody beads were injected into an embryo expressing Ana1-GFP (*green*) from the Ubq-promotor and Jup-mCh (MTs) (*magenta*). Time (mins:secs) is indicated and is relative to the first image (t=0:00), which was taken ~15-30mins after bead injection. This Movie remains centred on a single bead (*black asterisk*) within the embryo, that generates 3 CLiPs after the first round of mitosis, 2 of which duplicate after the next round of mitosis. Note that in these embryos Ana1-GFP is easily visible on the beads, but is barely visible at the centrioles or CLiPs, so centrosomes/CLiPs can only be visualised by the MTs they nucleate.

Movie S9.
Beads bound to GFP-Sas-6 can generate MTs and CLiPs. Anti-GFP-Nanobody beads, together with mRNA encoding GFP-Sas-6 (*green*), were injected into an embryo expressing Jup-mCh (MTs) (*magenta*). Time (mins:secs) is indicated and is relative to the first image (t=0:00), which was taken ~30-60mins after bead/mRNA injection. This approach was necessary as beads injected into embryos expressing GFP-Sas-6 from the Ubq-promoter did not efficiently generate MTs or CLiPs, so it was necessary to express Sas-6 at even higher levels by mRNA injection. This Movie remains centred on a single bead (*black asterisk*) within the embryo, that at the start of the movie appears to have previously generated 3 CLiPs that all duplicate once after a first round of mitosis, and then again after a second round of mitosis. Note that in these embryos GFP-Sas-6 is easily visible on the beads, but is barely visible at the centrioles/CLiPs, so centrosomes/CLiPs can largely only be visualised by the MTs they nucleate. Moreover, several additional beads are visible towards the top of the Movie that do not appear to generate MTs or CLiPs. Taken together, our data suggests that the ability of Sas-6-coupled-beads to induce MT/CLiP generation is lower than for beads coupled to the other centriole assembly proteins.

Movie S10.
Beads bound to GFP-Plk4 do not generate MTs or CLiPs. Anti-GFP-Nanobody beads were injected into an embryo expressing GFP-Plk4 (*green*) from the Ubq-promotor and Jup-mCh (MTs) (*magenta*). Time (mins:secs) is indicated and is relative to the first image (t=0:00), which was taken ~15-30mins after bead injection. This Movie remains centred on a single bead (*black asterisk*) within the embryo, and none of the beads in this Movie detectably generate any MTs or CLiPs. Note that in these embryos GFP-Plk4 is easily visible on the beads, but is not visible at the centrioles, so the centrosomes can only be visualised by the MTs they nucleate (*magenta*).

Movie S11.
Beads bound to Polo-GFP do not generate MTs or CLiPs. Anti-GFP-Nanobody beads were injected into an embryo expressing Polo-GFP (*green*) from its own promotor and Jup-mCh (MTs) (*magenta*). Time (mins:secs) is indicated and is relative to the first image (t=0:00), which was taken ~15-30mins after bead injection. This Movie remains centred on a single bead (*black asterisk*) within the embryo, and none of the beads in this Movie detectably generate any MTs or CLiPs. Note that in these embryos Polo-GFP is visible on the endogenous centrosomes and also on the kinetochores at the start of mitosis and on equatorial cortex and spindle midbody at the end of mitosis.

Movie S12.
Sas-6/Ana2-beads require Plk4 to generate CLiPs but not to generate MTs. Anti-GFP-Nanobody beads were injected into an embryo expressing Sas-6-GFP, Ana2-GFP (*green*) and Jup-mCh (MTs) (*red*) together with Plk4 RNAi. Time (mins:secs) is indicated and is relative to the first image (t=0:00), which was taken ~30-45mins after bead/RNAi injection. The centrosomes in this embryo (two highlighted with *white arrowheads*) had already stopped duplicating by the time the Movie starts. Hence, all the spindles that form around the chromatin during mitosis in this Movie have either only one or no endogenous centrosomes associated with them. The embryo continues to cycle despite the lack of centrosome duplication, and the remaining centrosomes and beads continue to organise MTs that cycle in synchrony with each other (being short in mitosis and longer in interphase). In these embryos, however, the centrioles cannot duplicate and the beads cannot generate CLiPs. Note that, due to the failure in centriole duplication, the actin caps and furrows that are normally organised by the centrosomes—and that stop nearby spindles from colliding with one another—are no longer formed properly. This means that the beads in Plk4 RNAi embryo can more easily access the mitotic chromatin and so form spindle poles. In this Movie, two beads (*black asterisks*) that are initially close together separate to form both poles of a spindle in the first round of mitosis. One of these beads then forms the pole of two spindles in the second round of mitosis.

Movie S13.
NG-Asl forms a torus around the barrel of mother centrioles and at CLiPs that can be visualised in living embryos by super-resolution microscopy. In this Movie, anti-ALFA-Nanobody beads were injected together with ALFA-Sas-6 and Ana2-ALFA mRNA into an embryo expressing NG-Asl (*green*) and Jup-mCh (MT marker) (*magenta*). Time (mins:secs) is indicated and is relative to the first image (t=0:00), which was taken ~30-45mins after bead injection. This Movie remains centred on a bead that generates a single CLiP (*cyan asterisk*) at the same time as an endogenous duplicated centriole (*white arrowhead*) separates at the end of mitosis. NG-Asl (*green*) forms a torus around the centrioles and CLiPs that can be visualised as either a ring (in an end-on view of the centriole/CLiP barrel) or a bar (in a side-on view of the centriole/CLiP barrel) on the SoRa super-resolution spinning disc system used here. The centrioles

and CLiPs move around in the embryo, flipping between end-on and side-on views of the NG-AsI torus.

Acknowledgements:
We thank members of the Raff Laboratory for many helpful discussions and comments.

Funding:
This work was funded by Wellcome Investigator (215523) and Discovery Awards (304037) (JWR, supporting CCC, MP, SSW, NM, JMM). CCC was supported by a National Science and Technology Council, Taiwan, Overseas Project for Postgraduate Research grant (111-2917-I-564-012). MP was supported by a National Science and Technology Council, Taiwan, Overseas Project for Postgraduate Research grant (114-2917-I-564-008) and by the Ministry of Science and Technology, Taiwan, Graduate Students Study Abroad Program (112-2917-I-002-026). SSW was supported by a Cancer Research UK Oxford Centre Prize DPhil Studentship (C5255/A23225), a Balliol College Jason Hu Scholarship, a Clarendon Scholarship, a Max Planck–Croucher Postdoctoral Fellowship, and a Junior Research Fellowship in Medical Sciences from Wadham College. JMM was supported by a Marie Skłodowska-Curie Individual Fellowship (892857, CENTROMD) from the European Commission and by an EMBO Long-Term Fellowship (LTF 29-2019).

Author Contributions:
CCC and MP contributed to conceptualization, methodology, investigation, resources, data curation, formal analysis, software, validation, visualization, project administration, supervision, writing—original draft, and writing—review & editing. LBM contributed to methodology, investigation, resources, data curation, validation, visualization, and writing—review & editing. SSW contributed to methodology, formal analysis, software, and writing—review & editing. NM contributed to resources. BX contributed to resources and writing—review & editing. JMM contributed to conceptualization and writing—review & editing. TH contributed to conceptualization. JWR contributed to conceptualization, methodology, investigation, resources, data curation, formal analysis, software, validation, visualization, project administration, supervision, writing—original draft, and writing—review & editing.

Competing interests:
The authors declare that they have no competing interests.

Data and materials availability:
All raw image data will be deposited at the Bioimage Archive upon acceptance. The custom Python scripts used to process images can be found via Zenodo (dOi: 10.5281/ zenodo.14202732). All data needed to evaluate the conclusions in the paper are present in the paper and/or the Supplementary Materials.